

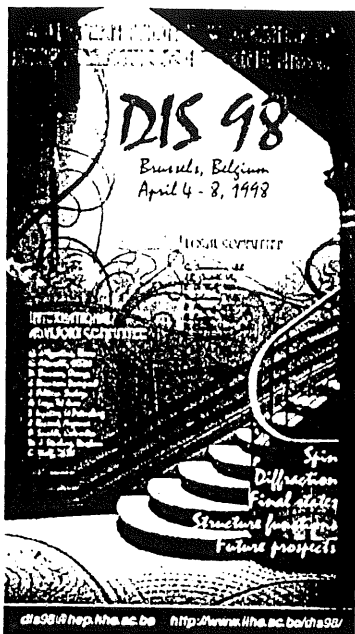
7TH INTERNATIONAL WORKSHOP ON
DEEP INELASTIC SCATTERING AND QCD
APRIL 19 - 23, 1999

P - 3

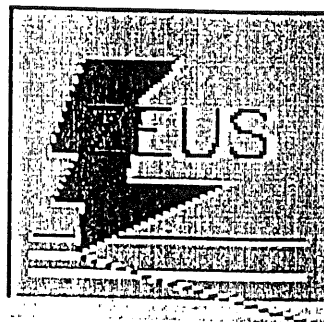
Results from the ZEUS Experiment

B. Loehr

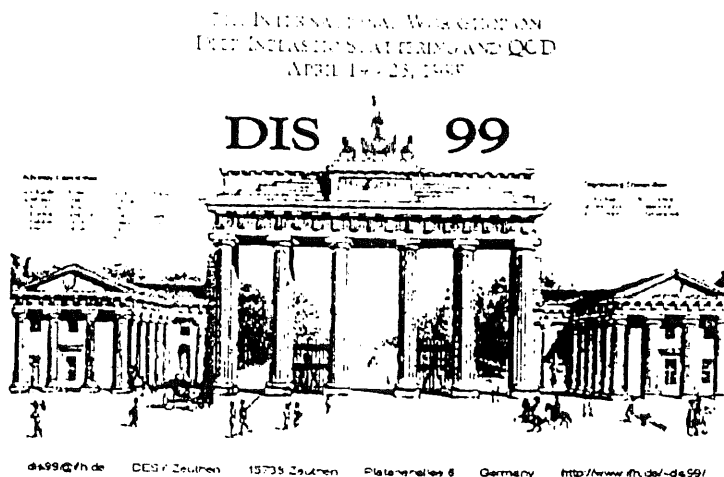
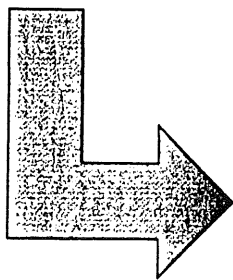
From DIS98



*Selected results
from*



to

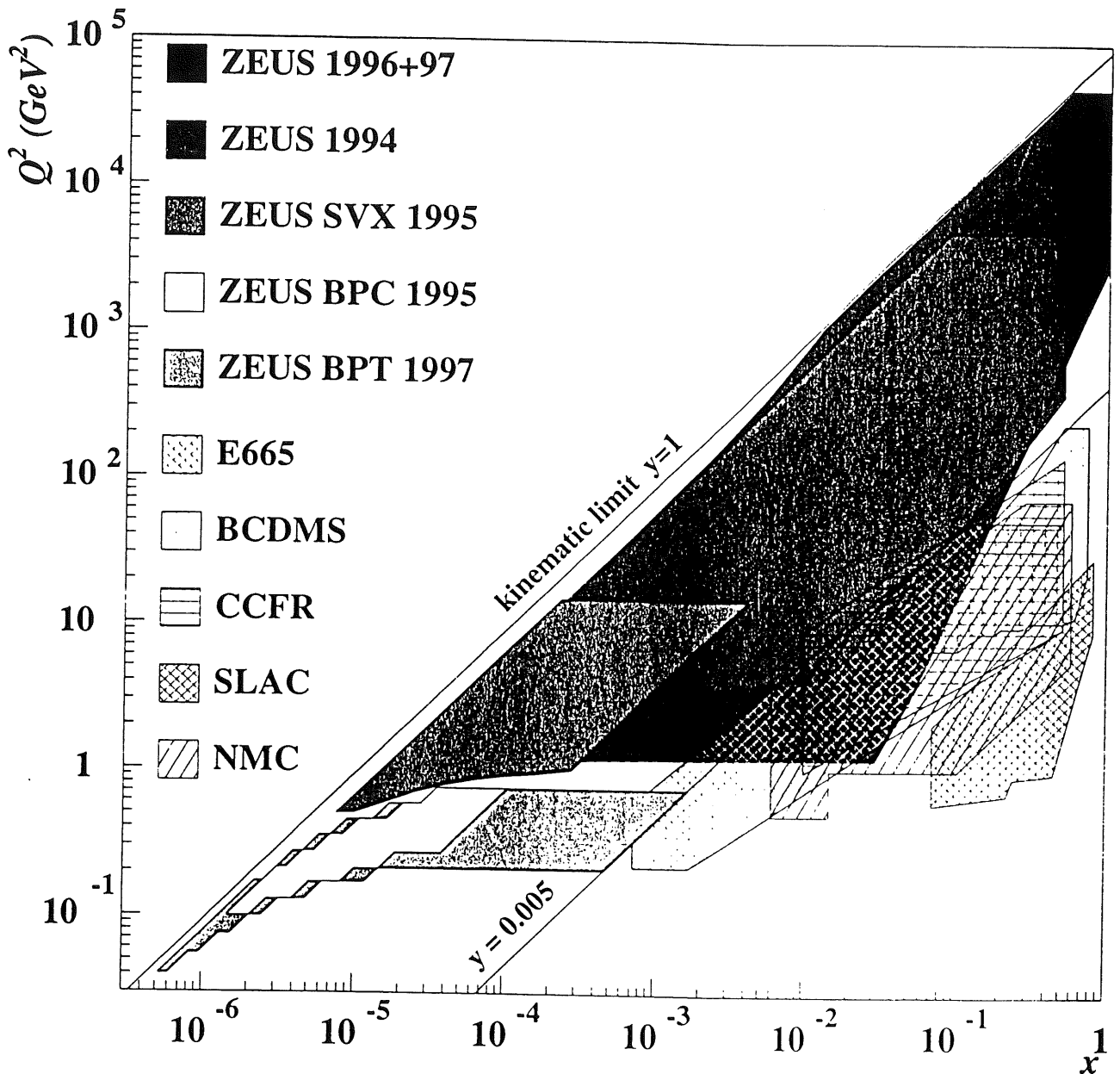


Presented by

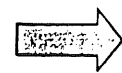
Bernd Loehr, DESY

DIS99 Zeuthen , April 19th, 1999

Inclusive Cross Section Measurements



Beam Pipe Tracker (BPT)
Beam Pipe Calorimeter



Very low Q^2

Increased statistics '96+'97

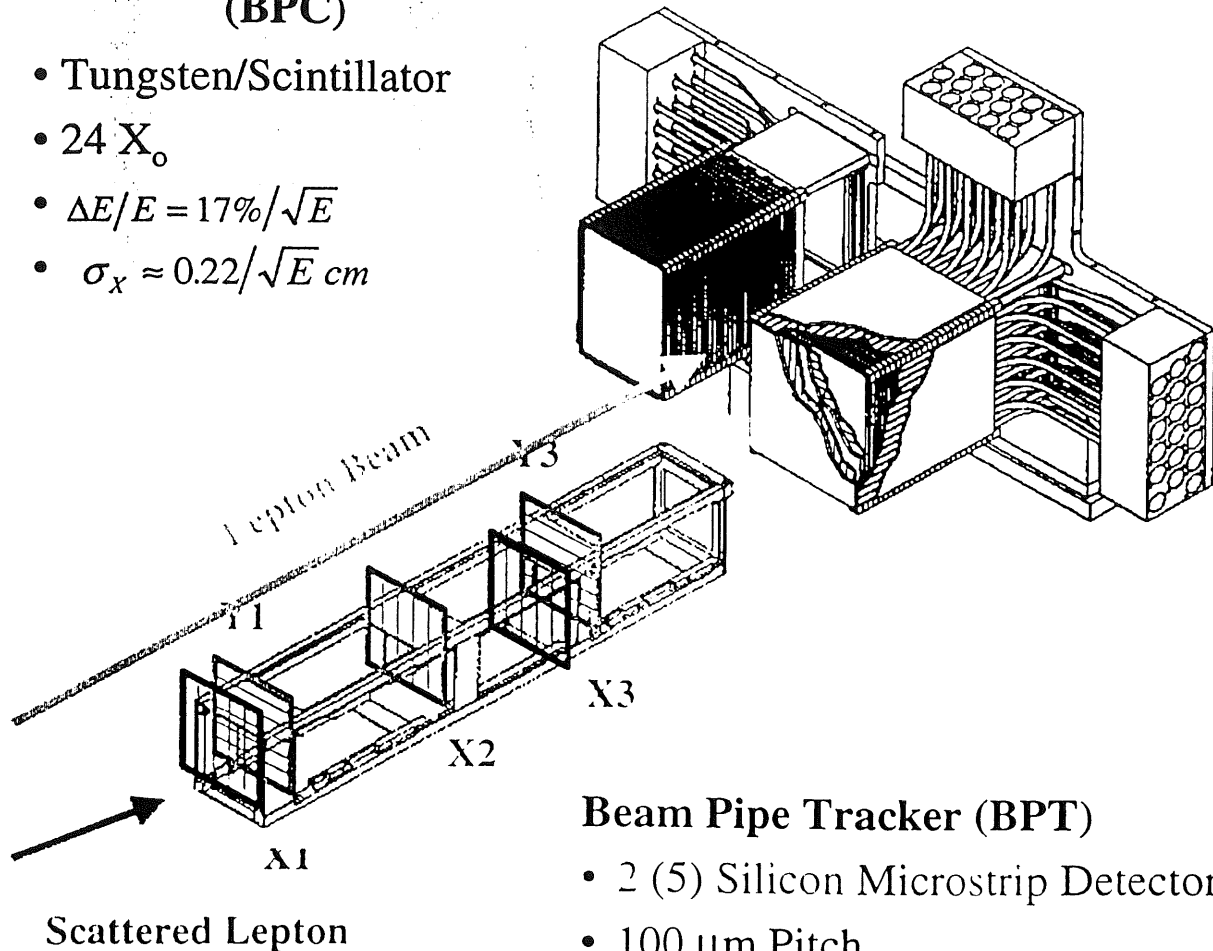


High Q^2

Beam Pipe Tracker (BPT) and BPC

Beam Pipe Calorimeter (BPC)

- Tungsten/Scintillator
- $24 X_0$
- $\Delta E/E = 17\%/\sqrt{E}$
- $\sigma_x \approx 0.22/\sqrt{E} \text{ cm}$

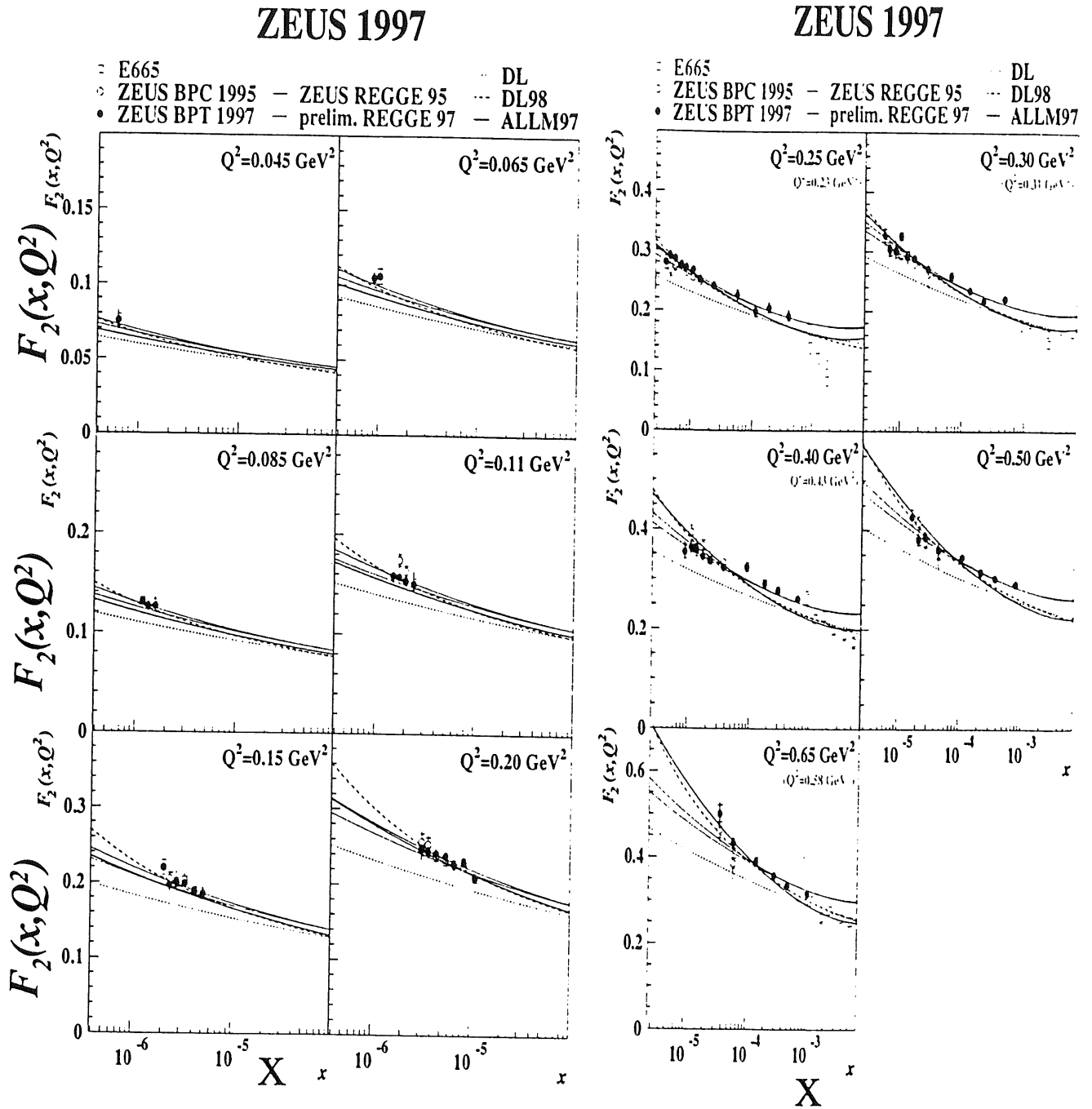


Beam Pipe Tracker (BPT)

- 2 (5) Silicon Microstrip Detectors
- $100 \mu\text{m}$ Pitch
- 2(3) planes in X, 0(2) planes in Y
- Efficiency for MIPS $> 99\%$
- Installed in 1997
- 3rd (X2) plane installed in 1998

BPT:- high accuracy in scattered e-angle
- much improved background rejection

F₂ from ZEUS BPT '97



Transition to $Q^2 = 0$

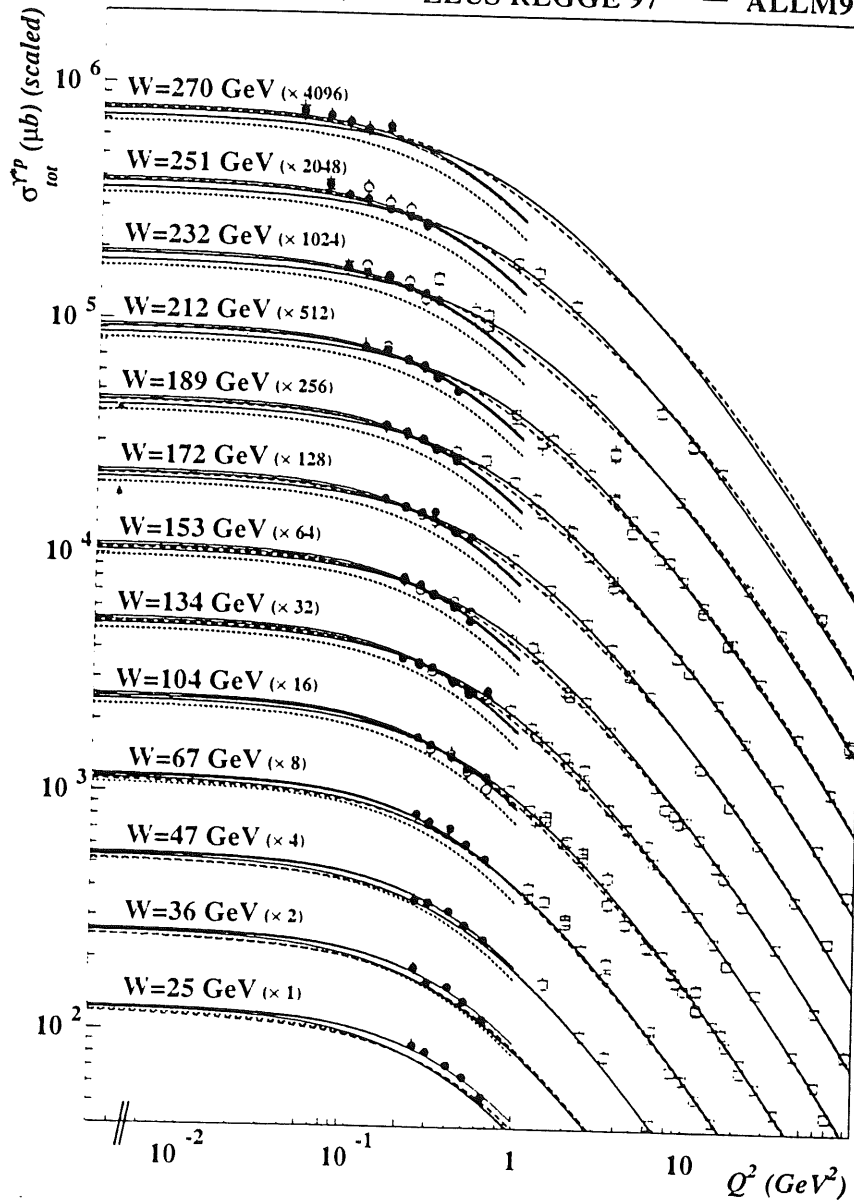
Regge fit describes data for

$Q^2 < 0.65 \text{ GeV}^2$

Total $\gamma^* p$ Cross Section

ZEUS 1997 (Preliminary)

- ZEUS+H1 94-95 ▲ ZEUS+H1 γp - - - DL
- ZEUS BPC 1995 — ZEUS REGGE 95 - - - DL98
- ZEUS BPT 1997 — ZEUS REGGE 97 — ALLM97

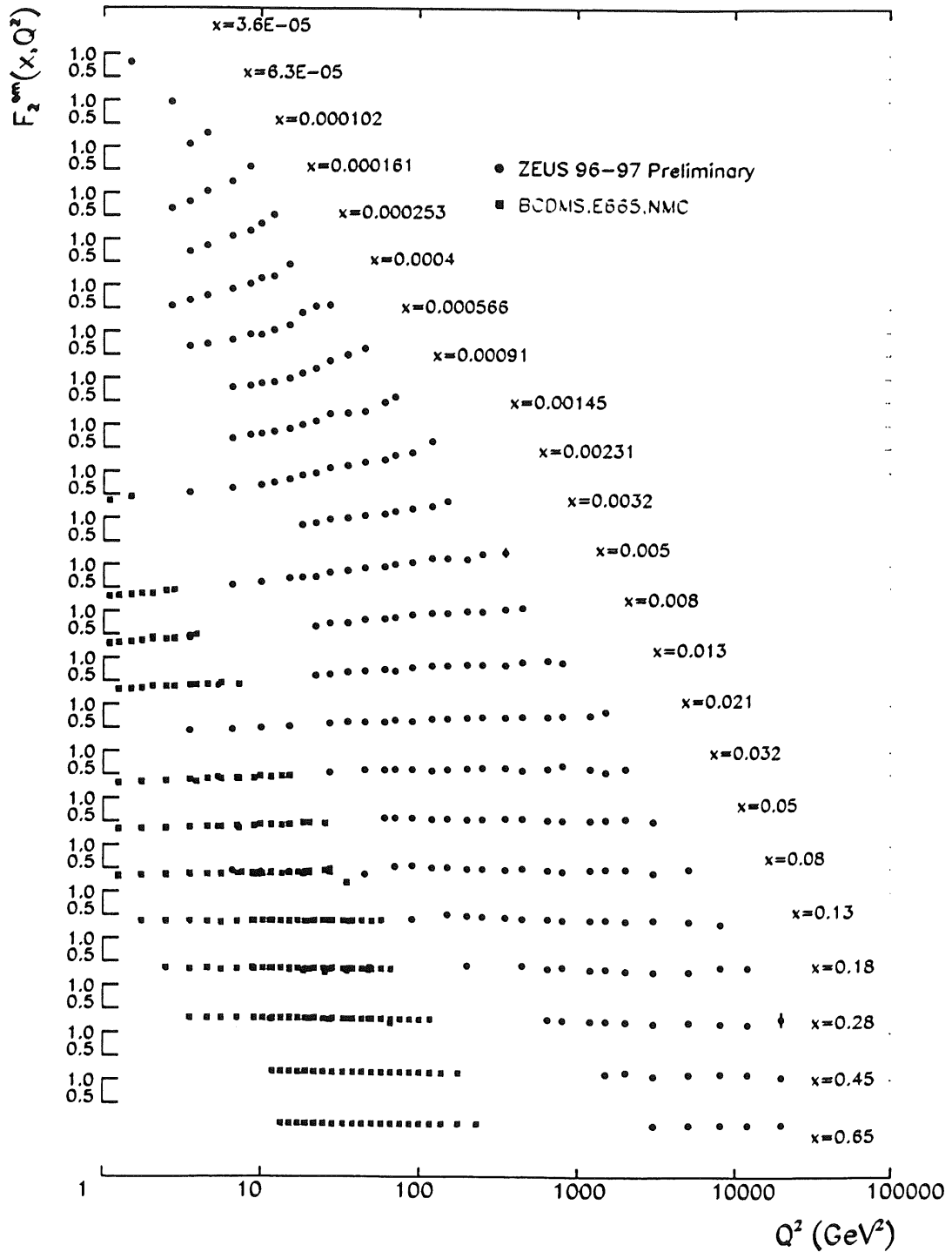


$$\sigma_{\text{tot}}^{\gamma^* p} = \frac{4\pi^2 \alpha}{Q^2} F_2$$

Extrapolate to $Q^2 = 0$ using GVDM and Regge parametrization :

$$\sigma_{\text{tot}}^{\gamma^* p}(W^2, Q^2) = \frac{m_0^2}{m_0^2 + Q^2} (A_R W^{-2(\alpha_R - 1)} + A_P W^{-2(\alpha_P - 1)})$$

Scaling Violations of $F_2(x, Q^2)$

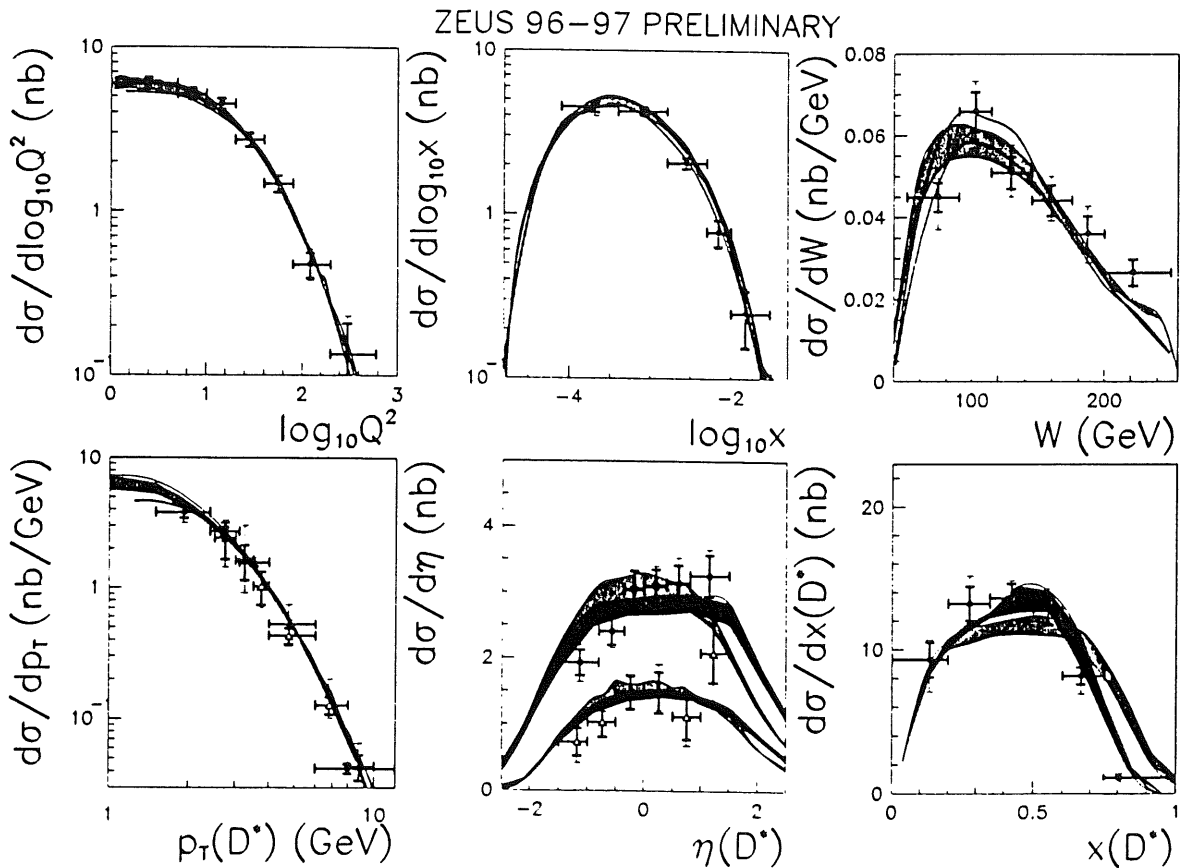
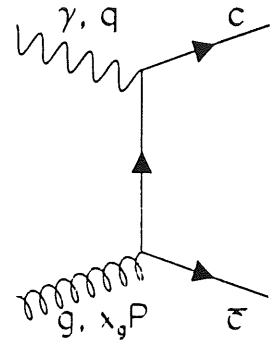


Charm in DIS

Charm production in DIS mainly through boson gluon fusion.

$$1 < Q^2 < 600 \text{ GeV}^2; \quad 0.02 < y < 0.715;$$

$$1.5 < p_T(D^*) < 15 \text{ GeV}; \quad |\eta(D^*)| < 1.5$$



Comparison with NLO Calculation :

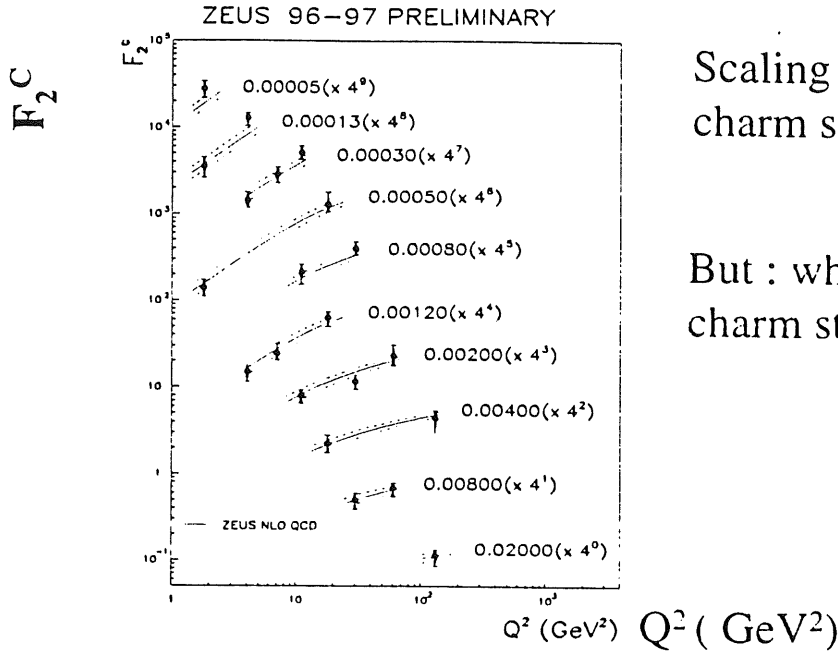
green band is HVQDIS, $m_c : 1.3 \text{ GeV} - 1.5 \text{ GeV}$

blue band is with fragmentation effects.

$$\sigma(e^+ p \rightarrow e^+ D^{*\pm} X) = 8.31 \pm 0.31(\text{stat}) \begin{matrix} +0.30 \\ -0.50 \end{matrix} (\text{sys}) \text{ nb}$$

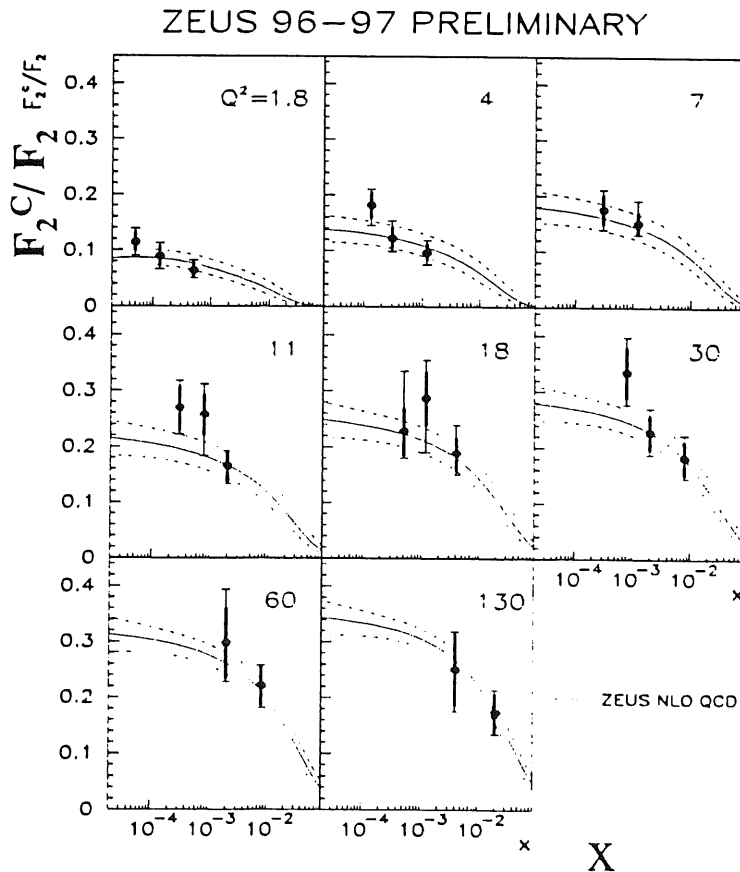
Charm Structure Function

Use HVQDIS to extrapolate from measured to full kinematical range in $p_T(D^*)$ and $\eta(D^*)$



Scaling violations in charm structure function

But : what is the charm structure function ?

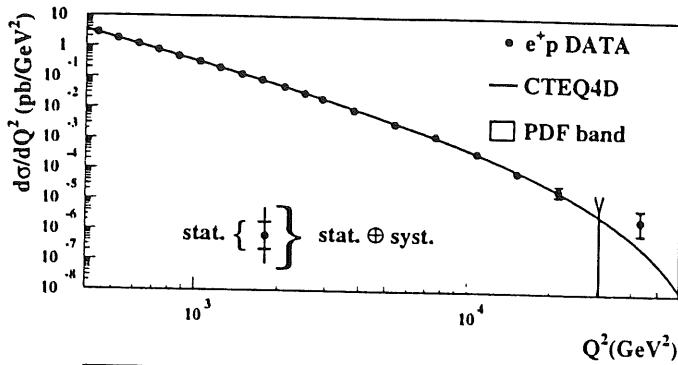


Fraction of charm increases with decreasing x .

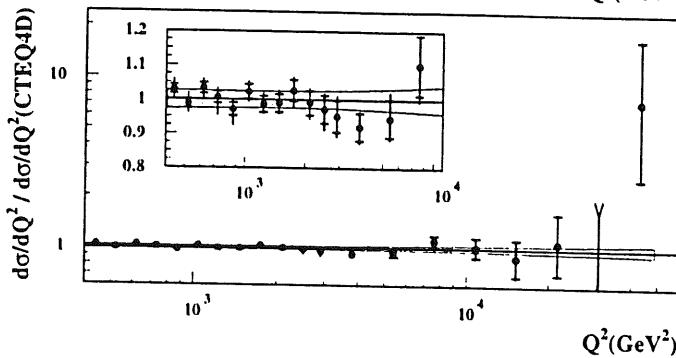
Contribution of charm in DIS grows with Q^2

NC and CC Cross Sections at High Q^2

ZEUS 1994 - 97

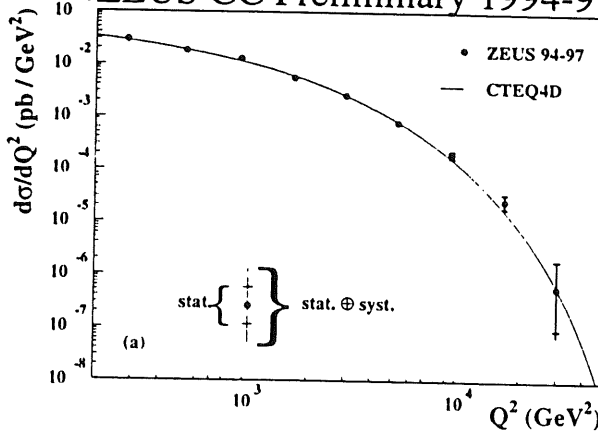


NC cross section compatible with Standard Model as in CTEQ4D

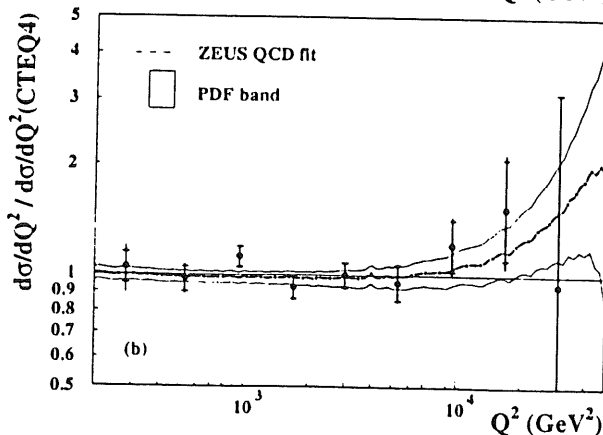


Maybe slight excess at highest Q^2

ZEUS CC Preliminary 1994-97



CC cross section compatible with Standard Model as in CTEQ4D



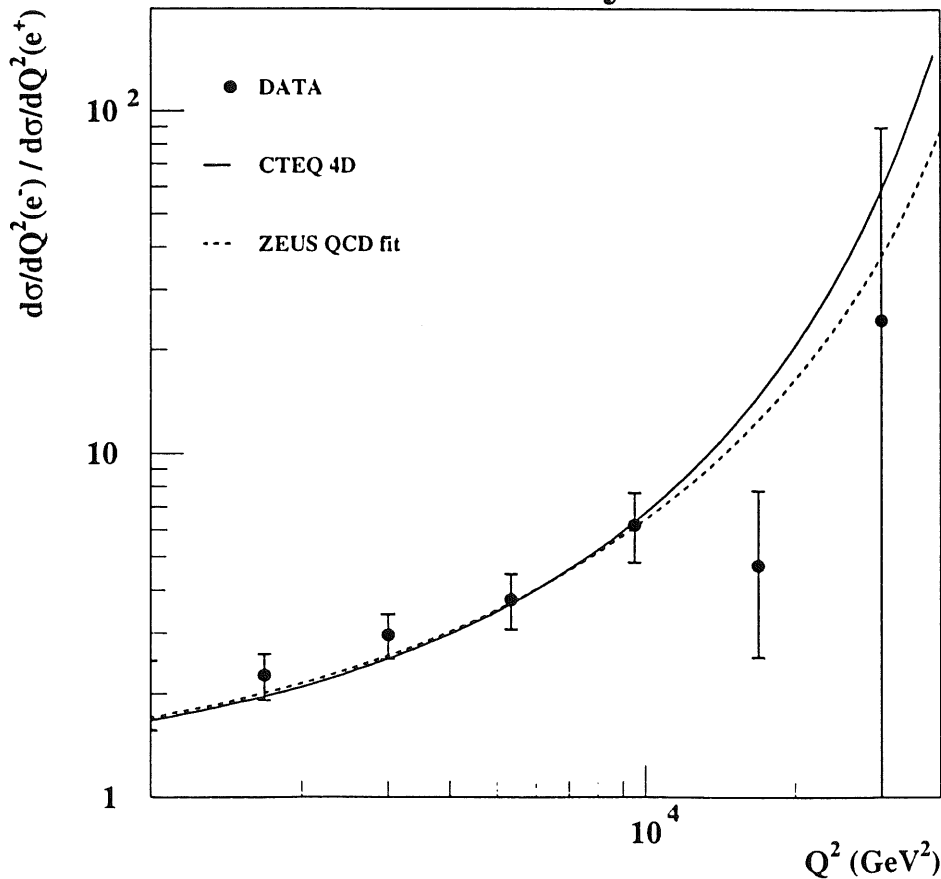
No sign of an excess at highest Q^2

CC Cross Section for e^+p and e^-p

$$\frac{d^2\sigma^{\text{CC}}(e^-p)}{dx dQ^2} \propto (u + c + (1-y)^2(\bar{d} + \bar{s}))$$

$$\frac{d^2\sigma^{\text{CC}}(e^+p)}{dx dQ^2} \propto ((1-y)^2(d + s) + \bar{u} + \bar{c})$$

ZEUS Preliminary 1998-99



e^+p data at
 $\sqrt{s} = 300 \text{ GeV}$

e^-p data at
 $\sqrt{s} = 318 \text{ GeV}$

Solid curve is prediction from CTEQ4D parametrization,
dashed curve is ZEUS fit.

$$M_W \text{ from } d\sigma^{\text{CC}} / dQ^2$$

$$\frac{d\sigma^{\text{CC}}}{dQ^2} = \frac{G_F^2}{4\pi} \frac{M_W^4}{(M_W^2 + Q^2)^2} F(Q^2)$$

Unconstrained fit to : $d\sigma^{\text{CC}} / dQ^2$

measurement of the spacelike $W \Rightarrow$ complementary to e^+e^- and pp measurements of timelike mass.

$$M_W = 80.9^{+4.9}_{-4.6} \text{ (stat)} \quad +5.0^{+1.3}_{-4.3} \text{ (syst)} \quad +1.3^{+1.3}_{-1.2} \text{ (pdf) GeV}$$

preliminary

Use Standard Model relation :

$$G_F = \frac{\pi\alpha}{\sqrt{2}} \frac{M_Z^2}{M_W^2 (M_Z^2 - M_W^2)} \frac{1}{1 - \Delta r(M_W)}$$

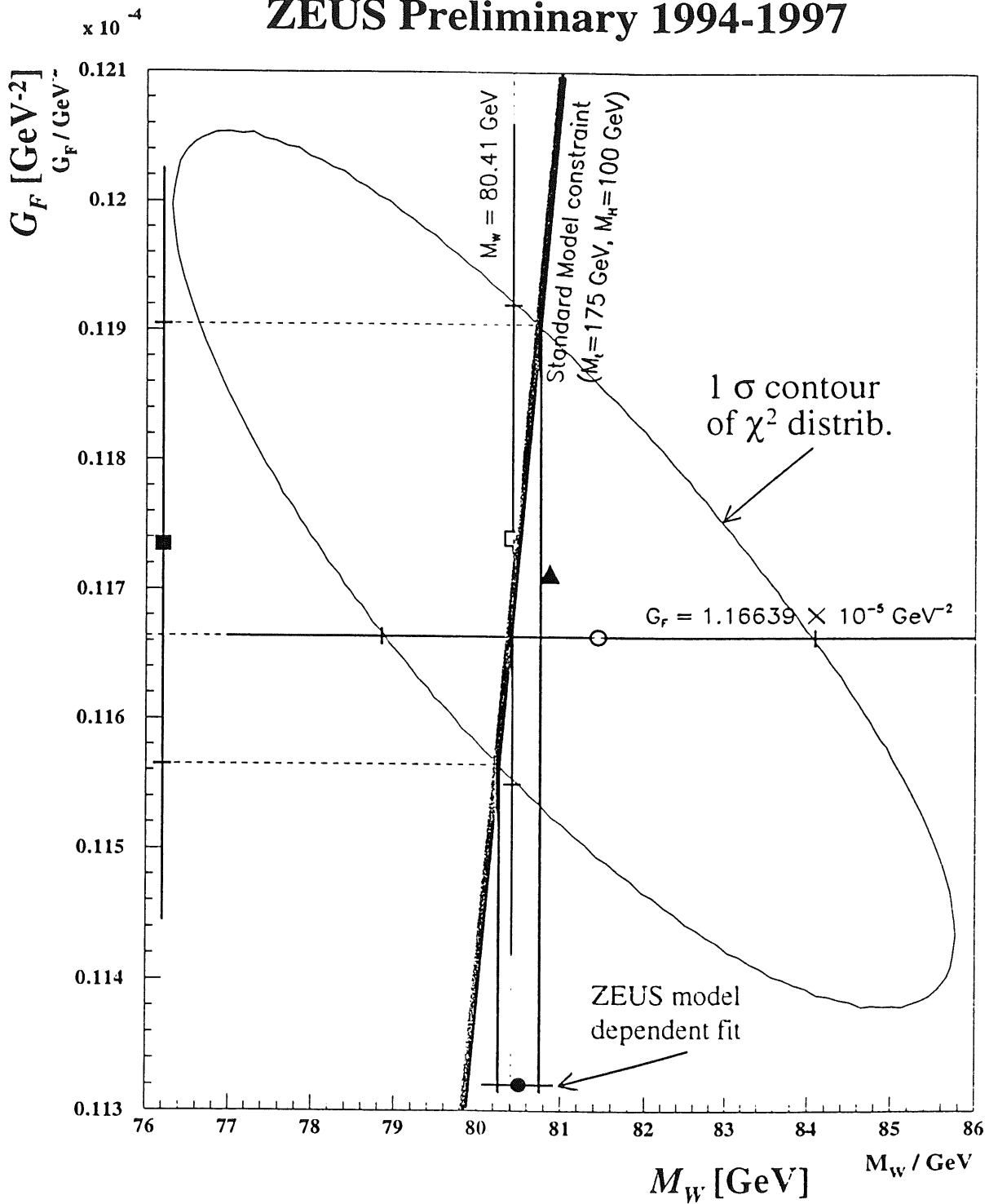
To exploit correlation between shape and normalization in a model dependent fit. Use $M_H = 100$ GeV , $M_T = 175$ GeV to extract M_W

$$M_W = 80.50^{+0.24}_{-0.25} \text{ (stat)} \quad +0.13^{+0.30}_{-0.16} \text{ (syst)} \quad +0.30^{+0.30}_{-0.31} \text{ (pdf) GeV}$$

Note: the last is not a measurement, but it indicates the sensitivity of the CC cross section to M_W assuming the validity of the Standard Model .

Sensitivity of G_F on M_W

ZEUS Preliminary 1994-1997



G_F depends very strongly on M_W
 \Rightarrow sensitivity to M_W

W Production

Selection of events from the reaction :

$$e^+p \rightarrow e^+W^\pm X; \quad W^\pm \rightarrow e^\pm\nu \text{ or } W^\pm \rightarrow \mu^\pm\nu$$

identified by requesting isolated lepton and missing p_T of more than 10 GeV.

3 events found in channel $W^+ \rightarrow e^+\nu$,
1 background event expected .

$$\sigma(e^+p \rightarrow e^+W^\pm X) = 0.9^{+1.0}_{-0.7} \text{ (stat)} \pm 0.2 \text{ (syst)} \text{ pb}$$

Search for Isolated Leptons at High p_T

Used event sample for W production to look for events with high missing transverse momentum and isolated leptons at high p_T .

3 events found with isolated positrons.

Expect from MC simulation of background :

3.4 ± 0.7 events for e^\pm and 1.9 ± 0.4 events for μ^\pm

No evidence for anomalous events

Search for Contact Interactions

Effective Lagrangian for eeq vector contact interactions

$$L_{CI} = \sum_{\alpha, \beta=L,R} \eta_{\alpha\beta}^{eq} \cdot (\bar{e}_{\alpha} \gamma^{\mu} e_{\alpha}) (\bar{q}_{\beta} \gamma_{\mu} q_{\beta})$$

$$\eta = \frac{\varepsilon \cdot g_{CI}^2}{\Lambda^2} \quad \text{where } \varepsilon = \pm 1 \quad \text{and by convention } g_{CI}^2 = 4\pi$$

Scalar and tensor terms are constrained beyond HERA sensitivity.

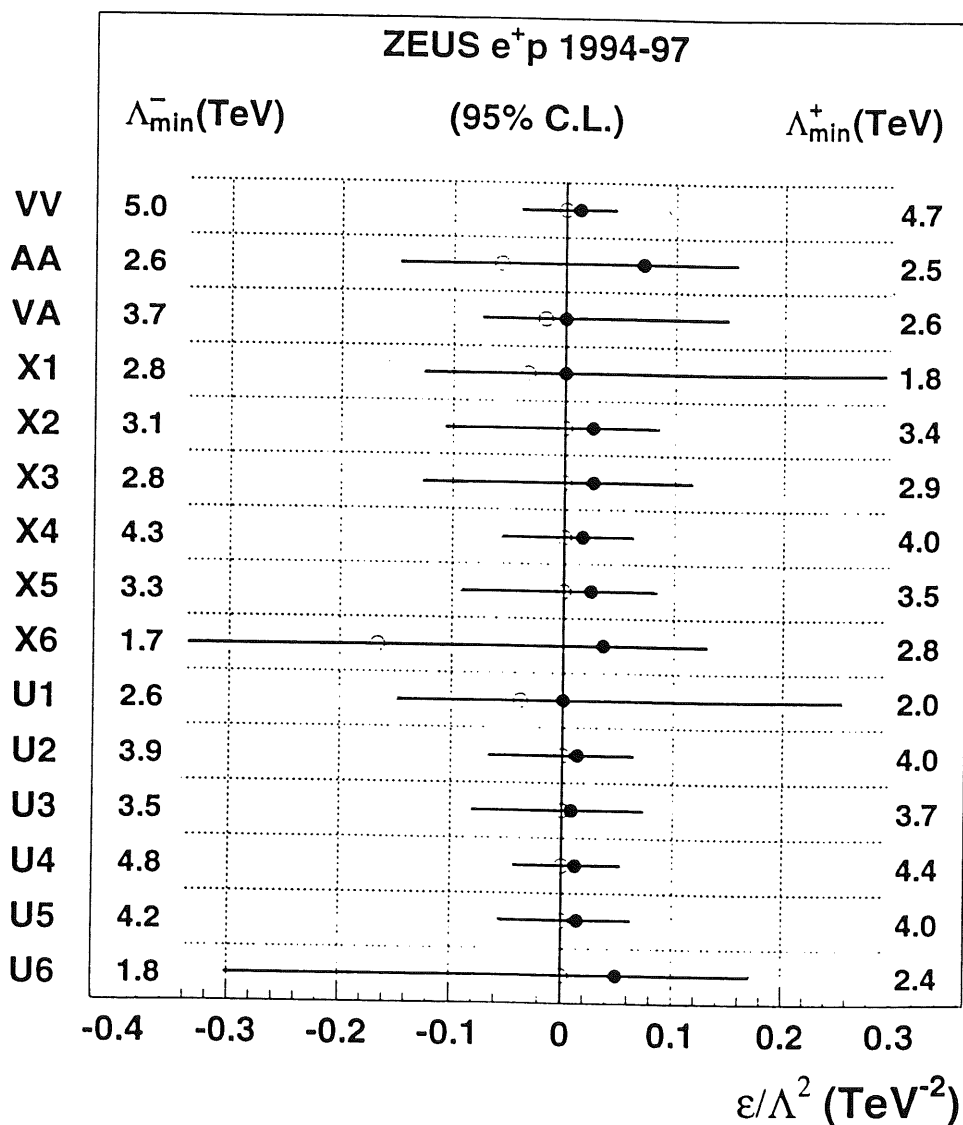
Assume quark flavor symmetry and parity conservation

$$\eta_{LL}^{eq} + \eta_{LR}^{eq} - \eta_{RL}^{eq} - \eta_{RR}^{eq} = 0$$

Model	η_{LL}^{ed}	η_{LR}^{ed}	η_{RL}^{ed}	η_{RR}^{ed}	η_{LL}^{eu}	η_{LR}^{eu}	η_{RL}^{eu}	η_{RR}^{eu}
VV	+ η	+ η	+ η	+ η	+ η	+ η	+ η	+ η
AA	+ η	- η	- η	+ η	+ η	- η	- η	+ η
VA	+ η	- η	+ η	- η	+ η	- η	+ η	- η
X1	+ η	- η			+ η	- η		
X2	+ η		+ η		+ η		+ η	
X3	+ η			+ η	+ η			+ η
X4		+ η	+ η			+ η	+ η	
X5		+ η		+ η	+ η			- η
X6			+ η	- η			+ η	- η
U1					+ η	- η		
U2					+ η		+ η	
U3					+ η			- η
U4						+ η	+ η	
U5						+ η		- η
U6							+ η	- η

Search for Contact Interactions

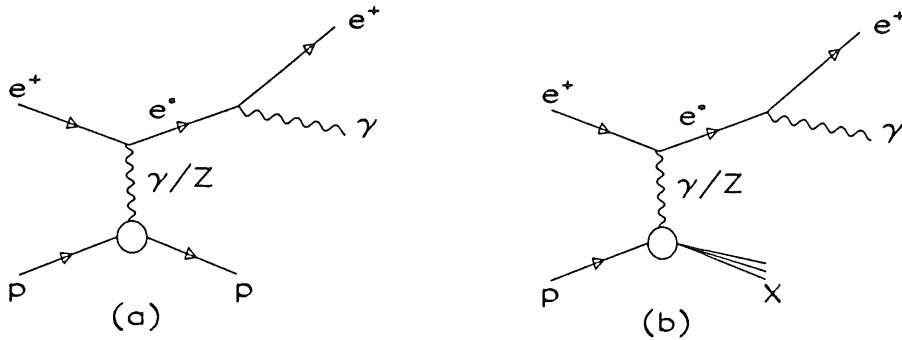
47.7 pb⁻¹ of high Q² data from NC reactions used to perform (standard model + CI) -fit.



Full points ● are best fits for $\eta(\epsilon=+1)$
 Open points ○ are best fits for $\eta(\epsilon=-1)$

Λ_{\min}^- (Λ_{\min}^+) are lower limits for $\epsilon = +1$ ($\epsilon = -1$)

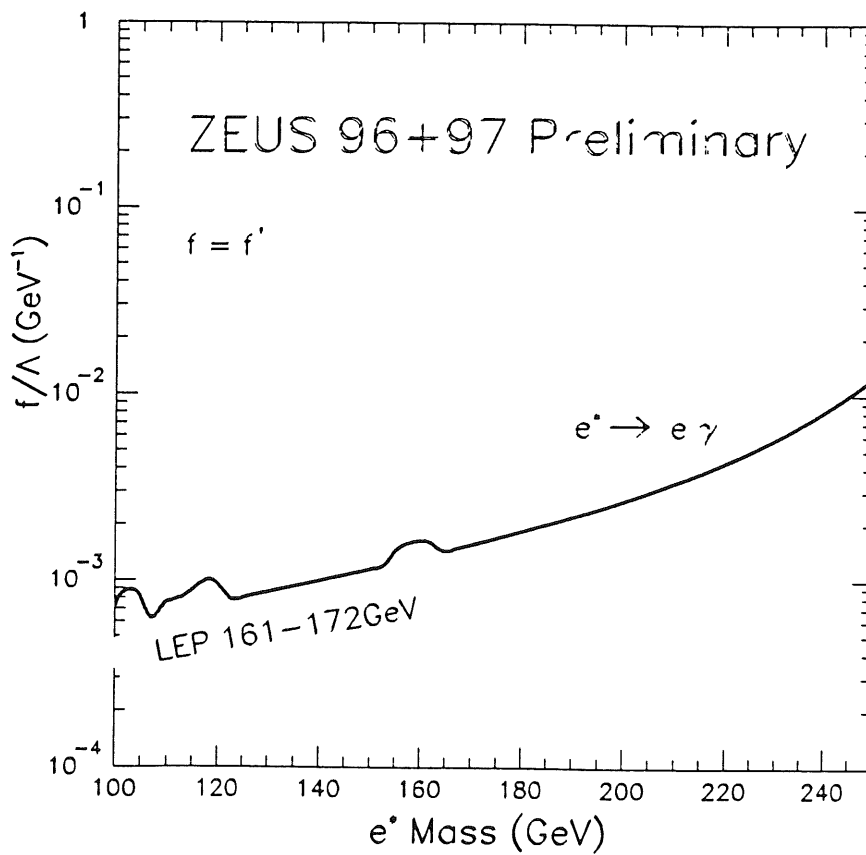
Search for Production of Excited Electrons



Searched for excited electrons in the $e^* \rightarrow e + \gamma$.

Calculate invariant mass of $(e + \gamma)$ - system with double angle method

7 events found with $(e + \gamma)$ - masses > 100 GeV, 8.8 expected



Resonance Search

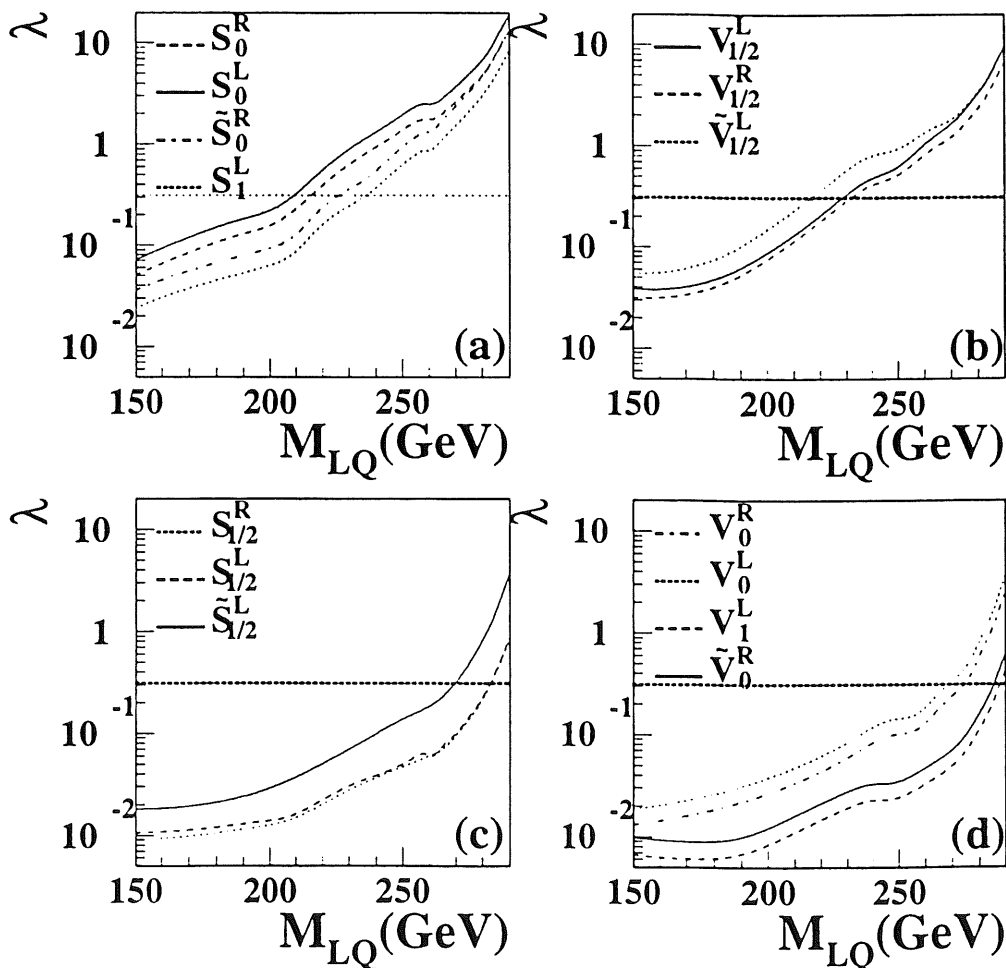
Search for $e\bar{p} \rightarrow LQ \rightarrow e + \text{jet}$

Select events with $E_e > 25$ GeV and $p_{T\text{-jet}} > 10$ GeV.

For $M_{ej} > 200$ GeV :
 68 events found
 43^{+14}_{-12} expected.

Angular distribution looks more like normal NC events than for heavy LQ decay.

ZEUS 1994-97 Preliminary



Search for R-Parity violating SUSY

Consequences of R_p violation ($R_p = (-1)^{3B+L+2S}$)

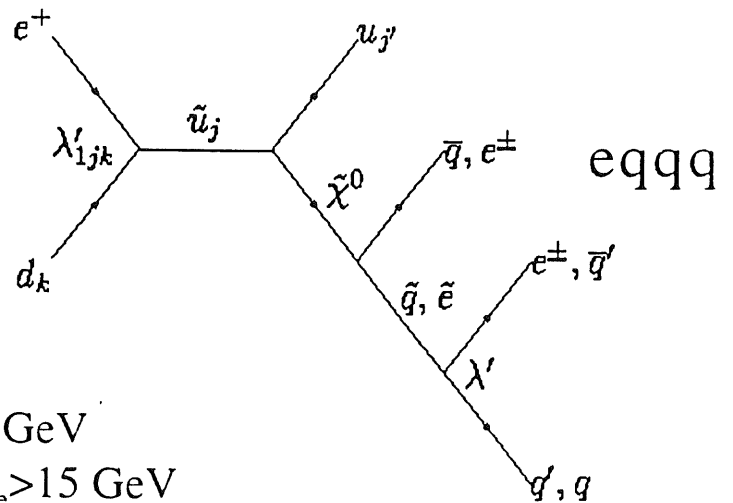
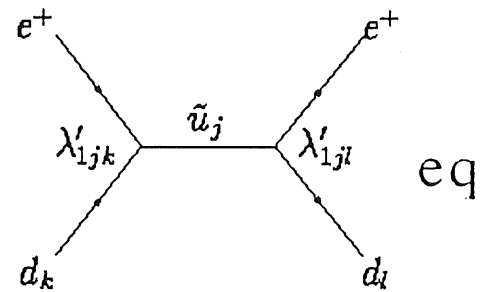
- sparticles can be singly produced
- LSP is not necessarily stable

⇒ eq and eqqq final states:

Only decay channels:

$\tilde{q} \rightarrow qe$ and $\tilde{q} \rightarrow q\tilde{\chi}^0$
are considered.

Data sample: 46.8 pb⁻¹



Selection:

eq: $E_t^{\text{jet}} > 30 \text{ GeV}, E_e > 15 \text{ GeV}$

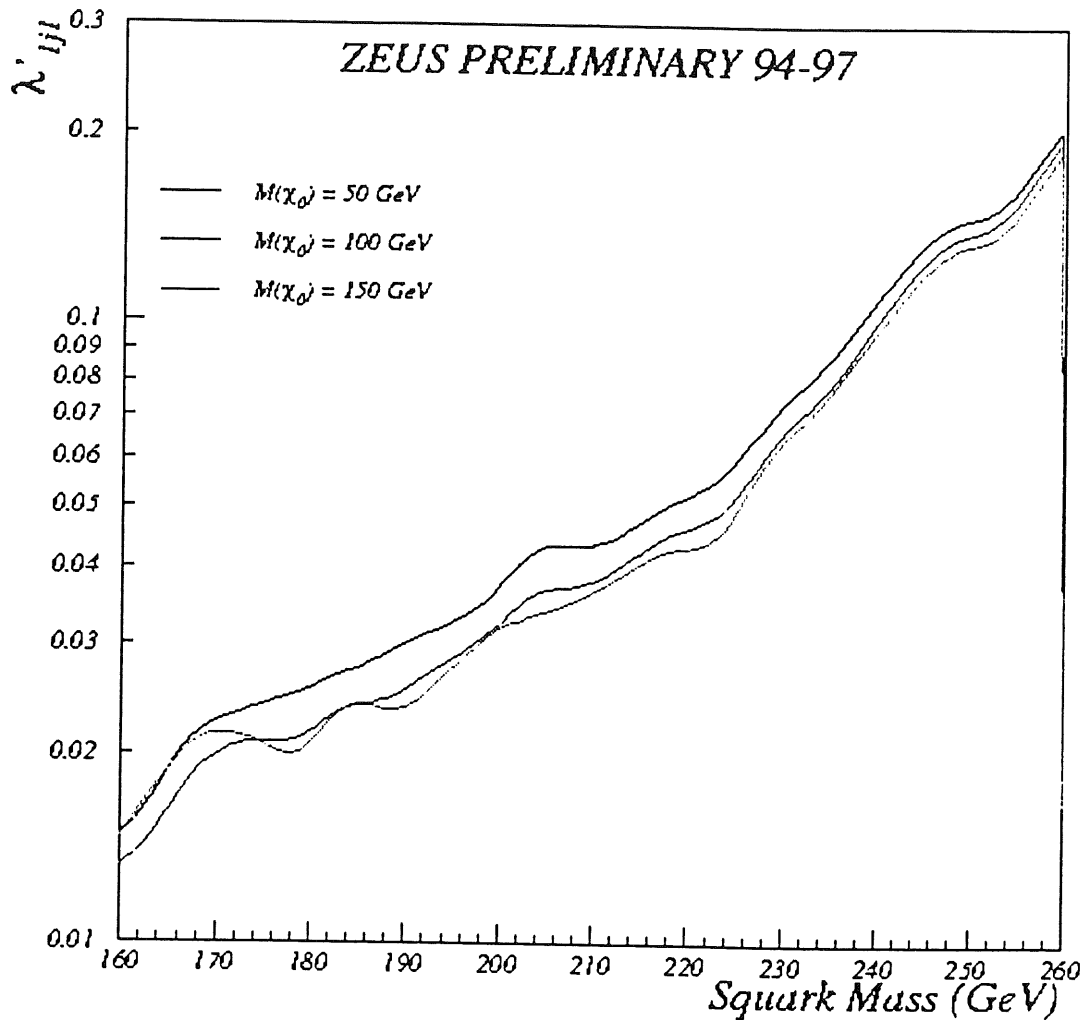
eqqq: $E_t^{\text{jet}1,2} > 40, 20 \text{ GeV}, E_e > 15 \text{ GeV}$

eq: 78 events found (88.6 exp.)

eqqq: 33 events found (33.6 exp.)

⇒ No evidence for squark production

Search for R-Parity violating SUSY (cont.)

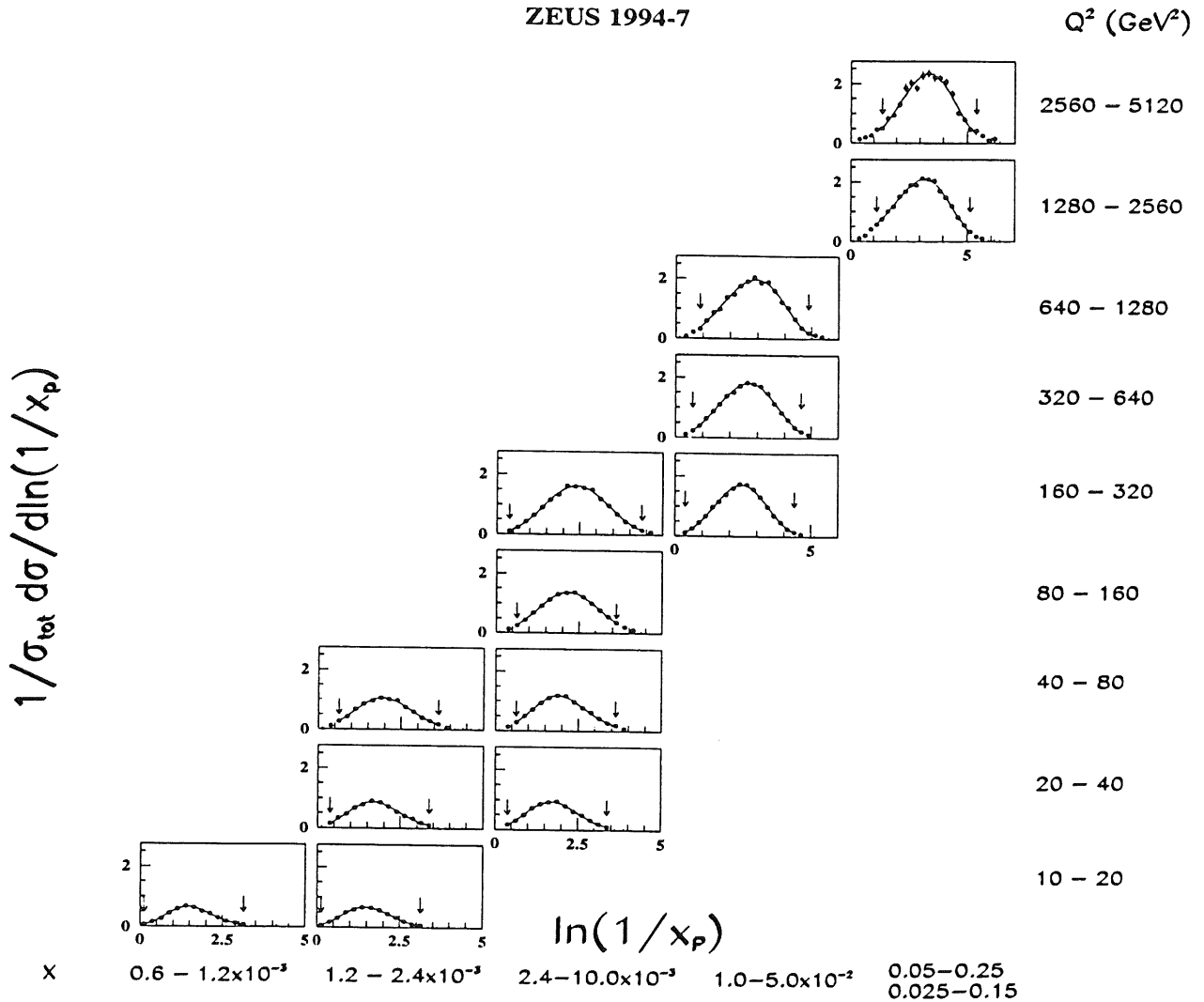


Preliminary limits on λ vs. squark mass range from below 0.02 at $\sim M_q = 160 \text{ GeV}$ to about 0.2 at $\sim M_q = 260 \text{ GeV}$

Fragmentation in DIS

Charged particle distributions in the current region of the Breit frame

$$\frac{1}{\sigma_{\text{tot}}} \frac{d\sigma}{d \ln(1/x_p)}, \quad x_p = 2p^{\text{Breit}} / Q$$



Full line : Fit of a distorted Gaussian, motivated by MLLA predictions

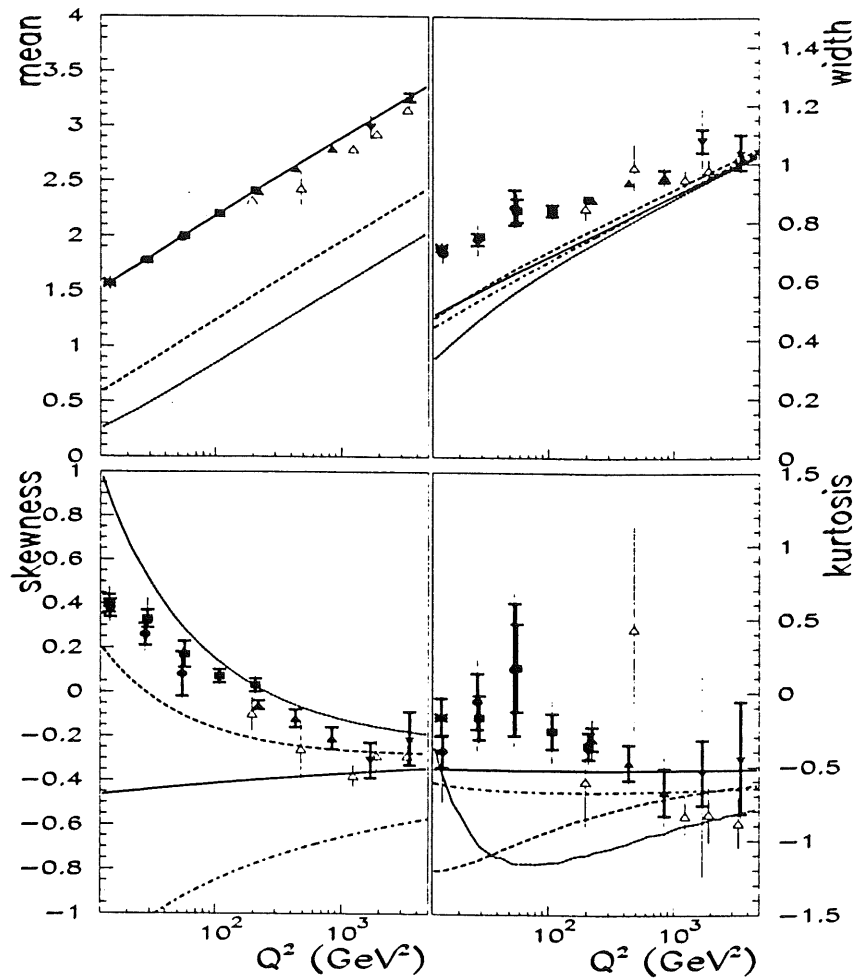
$$\frac{1}{\sigma_{\text{tot}}} \frac{d\sigma}{d \ln(1/x_p)} \propto \exp\left(\frac{1}{8}k - \frac{1}{2}s\delta - \frac{1}{4}(2+k)\delta^2 + \frac{1}{6}s\delta^3 + \frac{1}{24}k\delta^4\right), \quad \text{with } \delta = (\ln(1/x_p) - 1)/w$$

Where : l=mean, w=width, s=skewness, k=kurtosis

Fragmentation in DIS (cont.)

ZEUS 1994–1997

- | | |
|---|--|
| <ul style="list-style-type: none"> × $0.6 \cdot 10^{-3} < x < 1.2 \cdot 10^{-3}$ • $1.2 \cdot 10^{-3} < x < 2.4 \cdot 10^{-3}$ ■ $2.4 \cdot 10^{-3} < x < 10 \cdot 10^{-3}$ ▲ $1.0 \cdot 10^{-2} < x < 5 \cdot 10^{-2}$ | <ul style="list-style-type: none"> ▼ $0.025 < x < 0.15$ * $0.05 < x < 0.25$ △ e^+e^- |
|---|--|



Dokshitzer et al. :

full line $Q_0 = \Lambda$, dashed line $Q_0 = 2\Lambda$, dotted line $Q_0 = 3\Lambda$

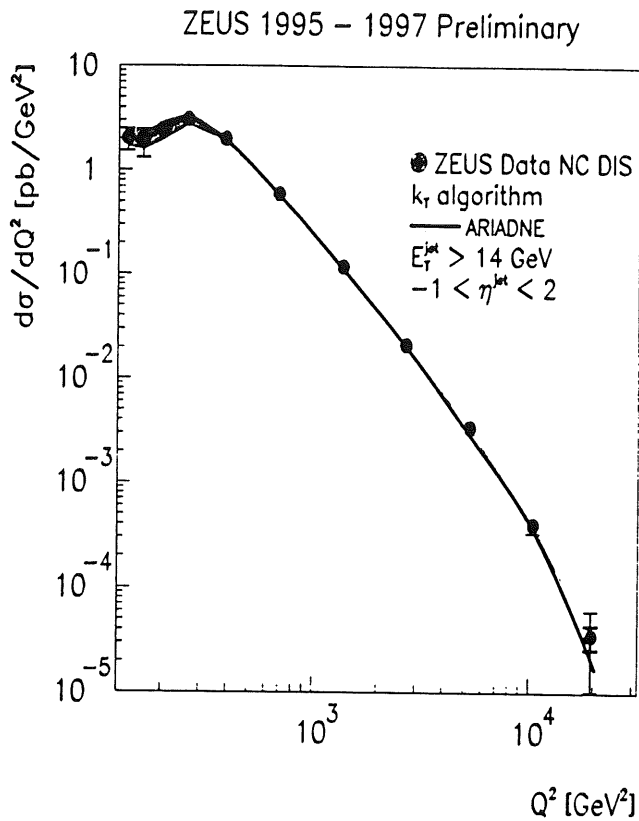
Fong an Webber : dashed-dotted line

No consistent description of the data, only mean is reproduced

Inclusive Single Jets in DIS

Updated analysis for single jet production in NC DIS from 42.5 pb^{-1}

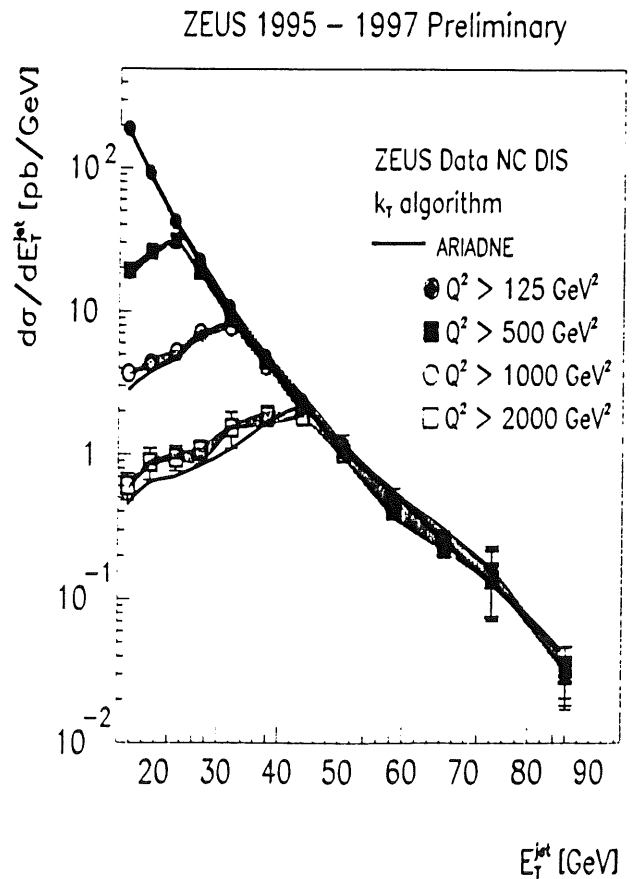
$$Q^2 > 125 \text{ GeV}^2 ; E_T^{\text{jet}} > 14 \text{ GeV}$$



Test of pQCD over
5 orders of magnitude

Slight discrepancy
for $Q^2 > 2000 \text{ GeV}^2$

This does not improve
when compared to NLO



Determination of α_s

Study of dijet production in NC DIS \Rightarrow pQCD applicable enables measurement of α_s

$$R_{2+1}(Q^2) = \frac{\sigma_{2+1}(Q^2)}{\sigma_{\text{tot}}(Q^2)} ; \quad \sigma_{2+1}(Q^2) = c_1 \cdot \alpha_s(Q^2) + c_2 \cdot \alpha_s^2(Q^2) + \dots$$

Select dijet events with :

$$Q^2 > 470 \text{ GeV}^2 ; \quad -1 < \eta^{\text{jet}} < 2 \text{ (Lab. frame)}$$

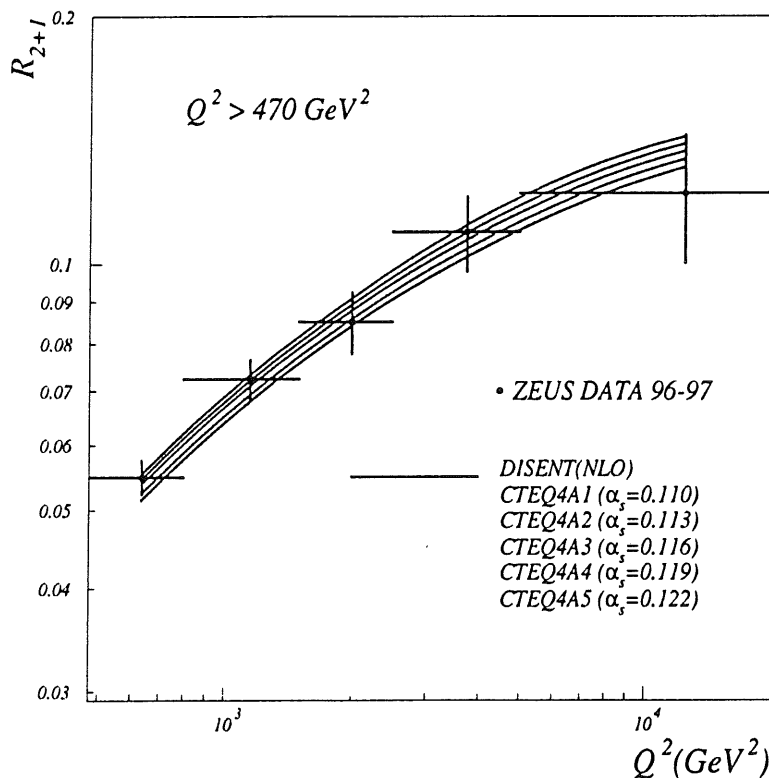
$$E_T^{\text{jet1}}, E_T^{\text{jet2}} > 5 \text{ GeV} ; \quad E_T^{\text{jet1}} + E_T^{\text{jet2}} > 17 \text{ GeV (Breit frame)}$$

Region of
small
experimental
and theoretical
uncertainties

Compare measured dijet ratio to NLO calculations (DISENT)

$$\underline{R_{2+1}}$$

ZEUS 96-97 PRELIMINARY



$$\alpha_s(M_Z) = 0.120 \pm 0.003 \text{ (stat.) } \begin{matrix} +0.005 \\ -0.006 \end{matrix} \text{ (exp.) } \begin{matrix} +0.003 \\ -0.002 \end{matrix} \text{ (theory)}$$

Photon Structure as Function of Q^2

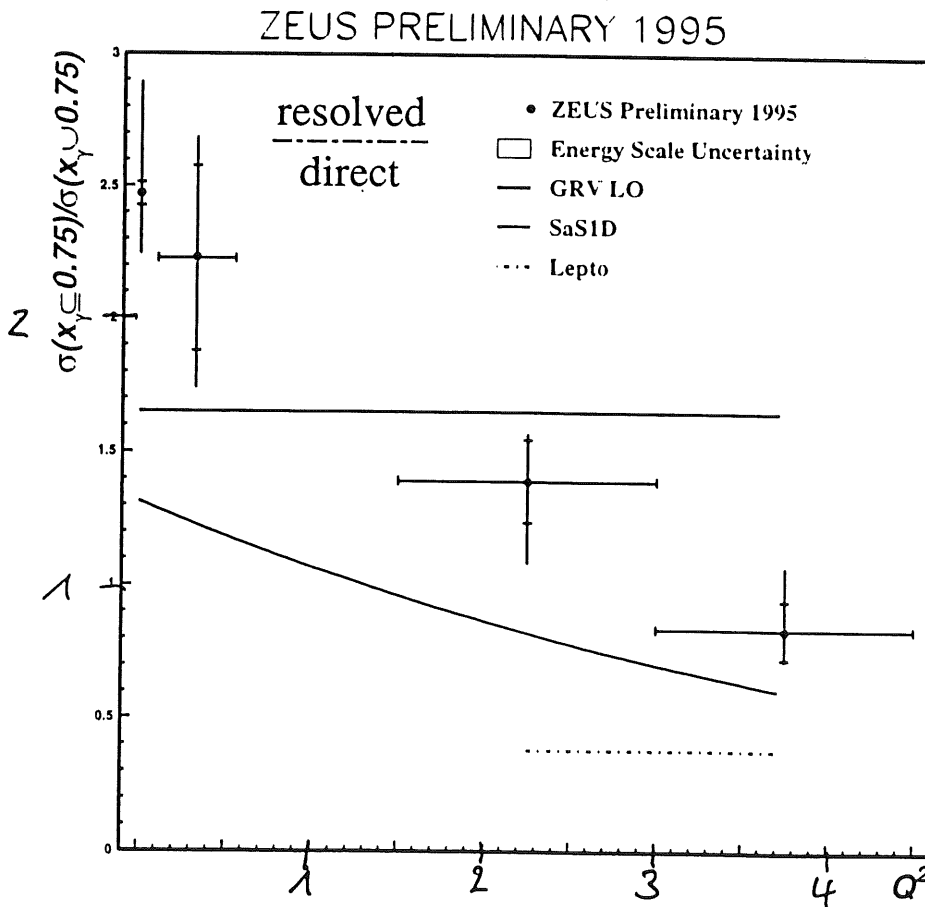
The photon can couple directly to quarks or fluctuate into partons, one which then interacts with the proton.

$$x_\gamma^{\text{obs}} < 0.75 \quad x_\gamma^{\text{obs}} = \frac{\sum_{\text{jets}} E_T e^{-\eta}}{2yE_e} \cong \frac{(E - p_z)_{\text{jets}}}{(E - p_z)_{\text{total}}} \quad x_\gamma^{\text{obs}} > 0.75$$

Resolved enriched sample

Direct enriched sample

Direct contribution : no dependence on Q^2



VDM component :

$$\left(\frac{m_V^2}{(m_V^2 + Q^2)} \right)^2$$

pQCD component :

$$\ln \left(\frac{E_T^2}{Q^2} \right)$$

Direct contribution is expected to become small at high Q^2

Curves : HERWIG — GRV, — SaS ; - - - LEPTO

Dijet Photoproduction at High E_T

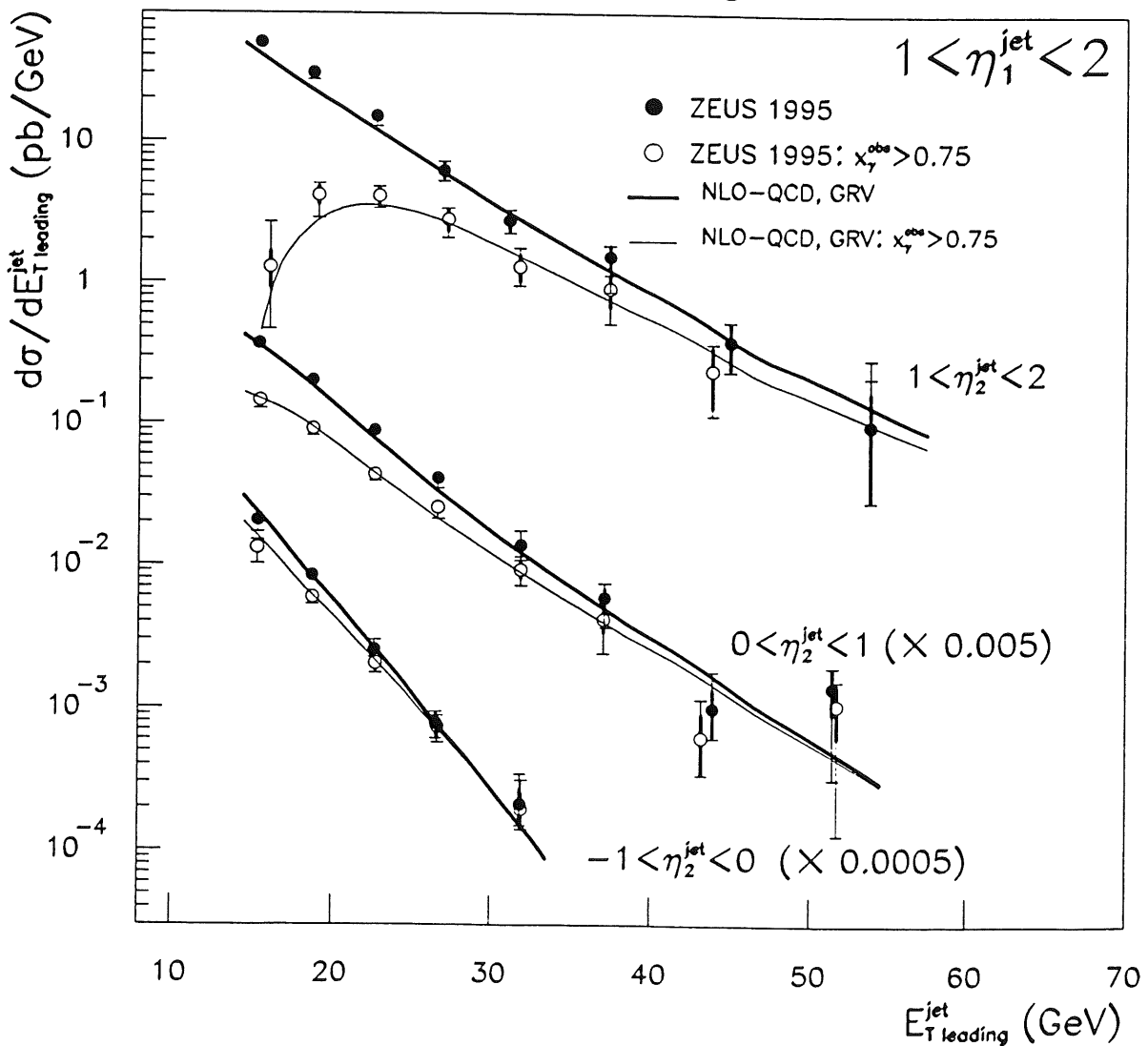
When $(E_T^{\text{jet}})^2 \gg Q^2$ the dijet system probes the photon structure .

Dataset : at least 2 jets with $E_{T,\text{leading}}^{\text{jet}} > 14 \text{ GeV}$ and $E_{T,\text{second}}^{\text{jet}} > 11 \text{ GeV}$

$x_{Bj} \approx 10^{-2} - 10^{-1}$ $Q^2 < 1 \text{ GeV}^2$, and $0.20 < y < 0.85$

=> parton densities well restricted in this region.

ZEUS 1995



In general, NLO describes data, but in forward direction at $E_{T,\text{leading}}^{\text{jet}} < 25 \text{ GeV}$ data lie above NLO predictions.

Subjects in Photoproduction

Quark and gluon jets are expected to be different due to different qg and gg couplings.

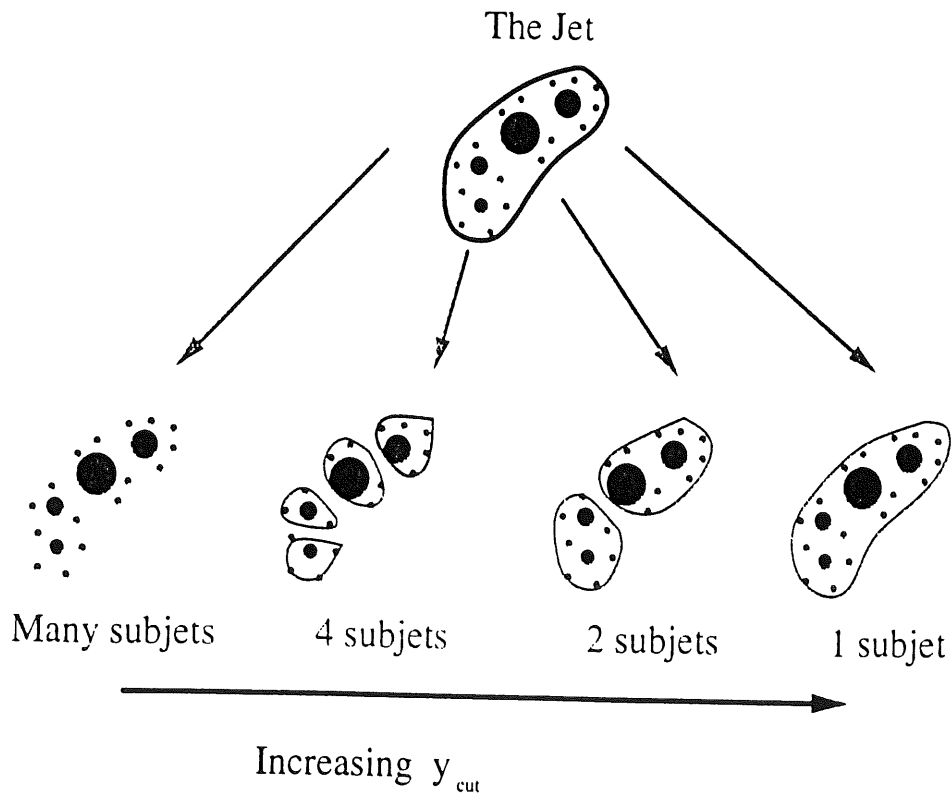
Investigate structure of jets by looking for subjects.

- First find jets with k_T cluster algorithm
- Re-run k_T cluster algorithm on all particles within one jet and stop when

$$d_{ij} = \min(E_T^i, E_T^j)^2 \cdot (\Delta\eta_{ij}^2 + \Delta\phi_{ij}^2) \quad \text{are above}$$

$$d_{\text{cut}} = y_{\text{cut}} \cdot (E_T^{\text{jet}})^2$$

Remaining objects are subjects as functions of y_{cut} .

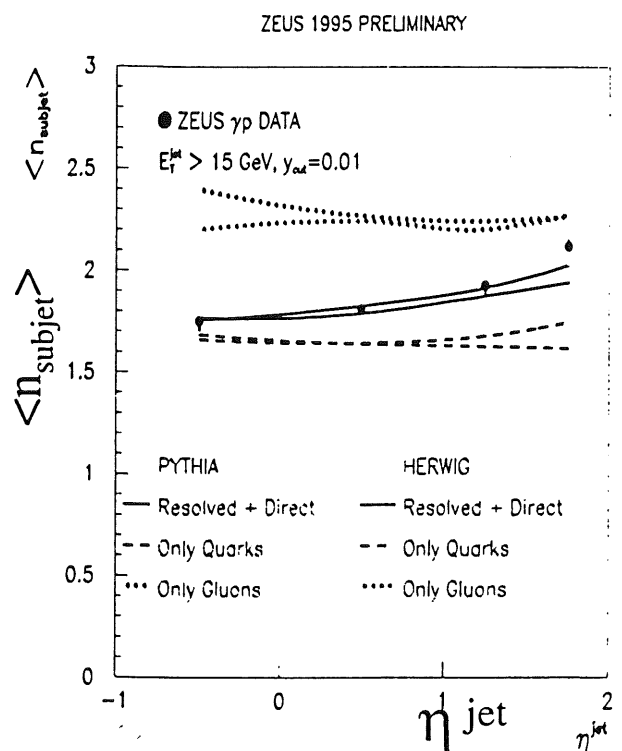
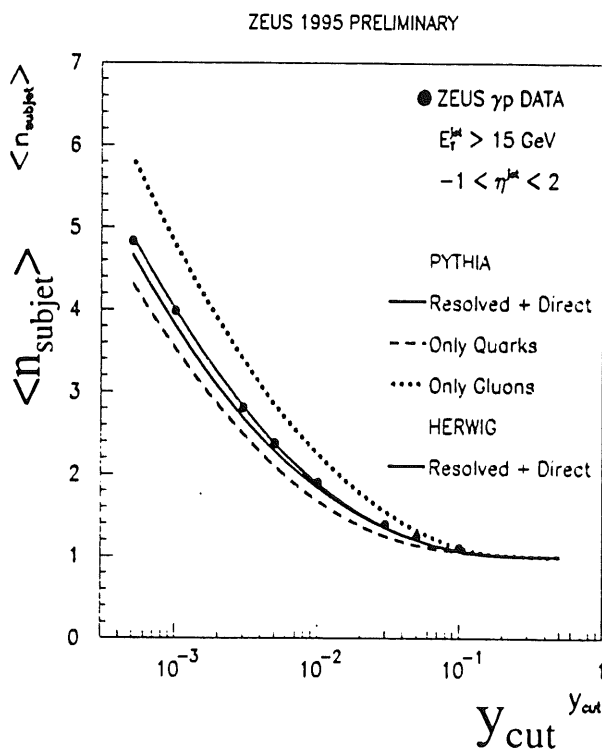


Subjects in Photoproduction (cont.)

$$Q^2 < 1 \text{ GeV}^2 ; E_T^{\text{jet}} > 15 \text{ GeV}^2 ; -1 < \eta^{\text{jet}} < 2 \rightarrow > 10^4 \text{ jets}$$

Count average number of subjects, $\langle n_{\text{subject}} \rangle$, as function of y_{cut}

Plot $\langle n_{\text{subject}} \rangle$ as function of η_{jet} for a fixed value of y_{cut}



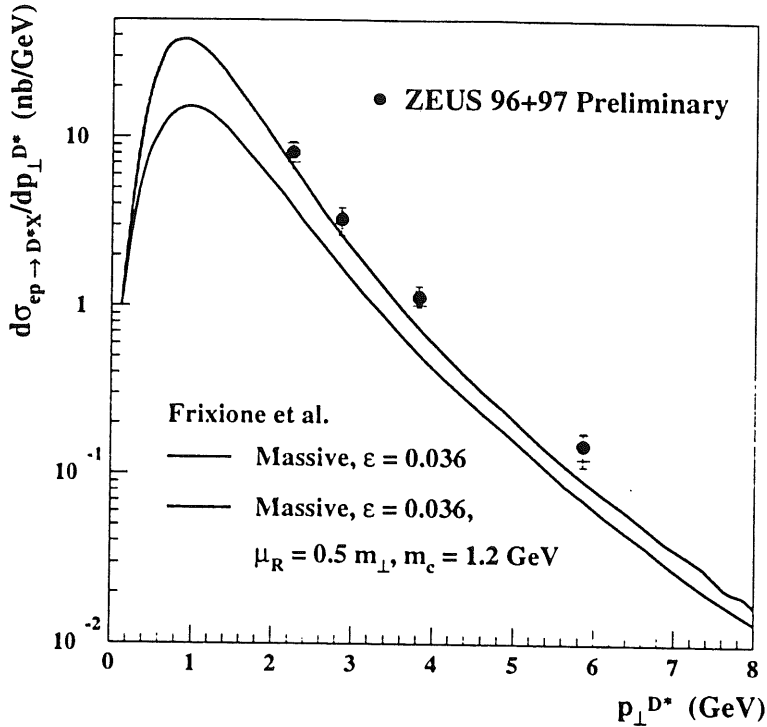
Direct (boson-gluon fusion) produces 2 quarkjets,
dominates in backward direction.

Resolved processes produce also gluon jets
dominate in forward direction.

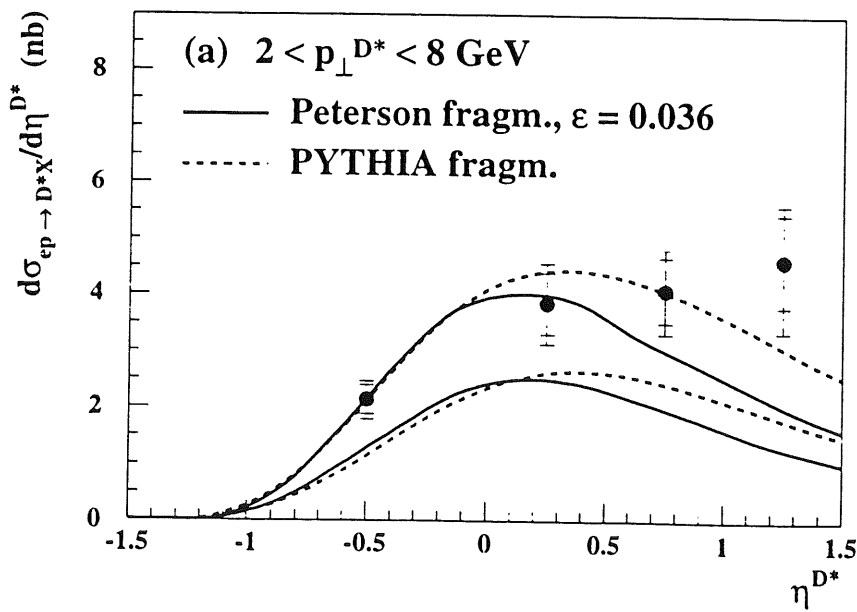
Photoproduction of Charm

New data on low W production of D^* mesons

Differential cross sections

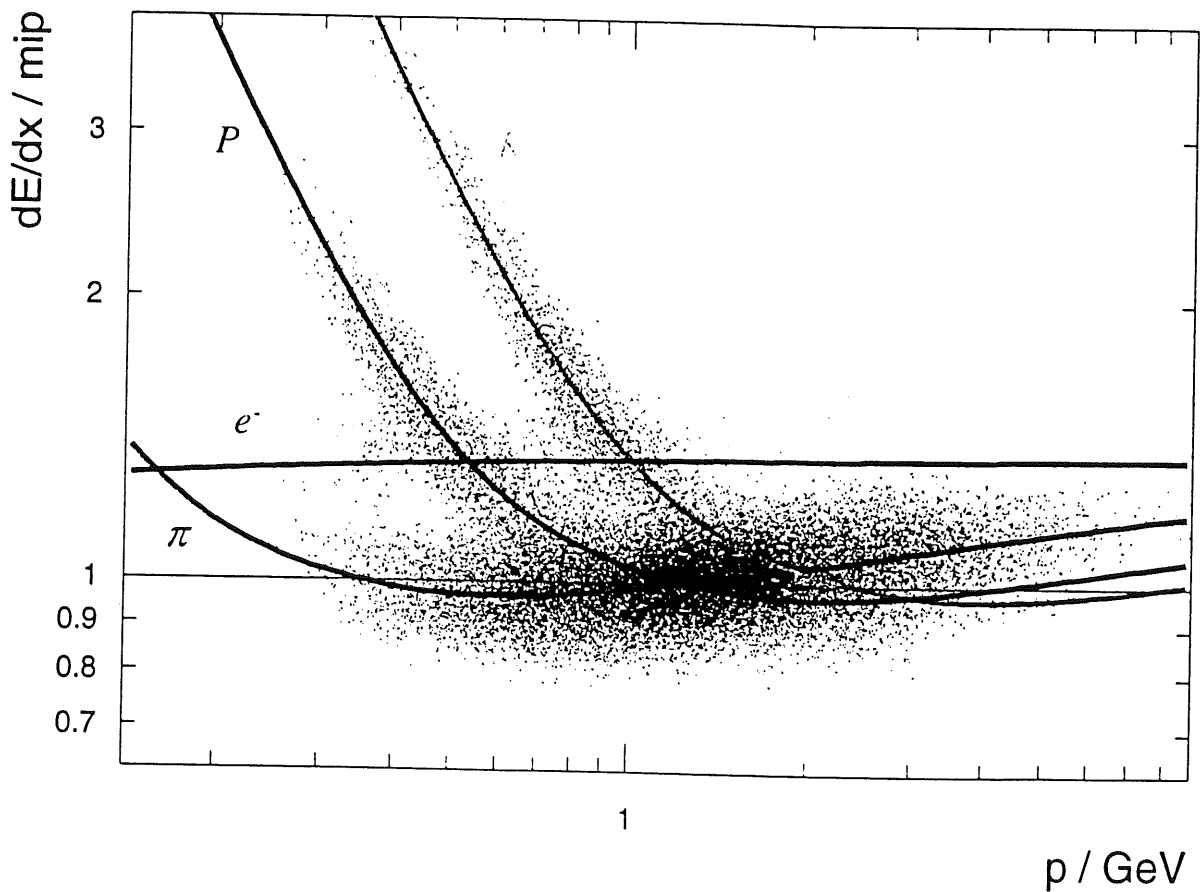
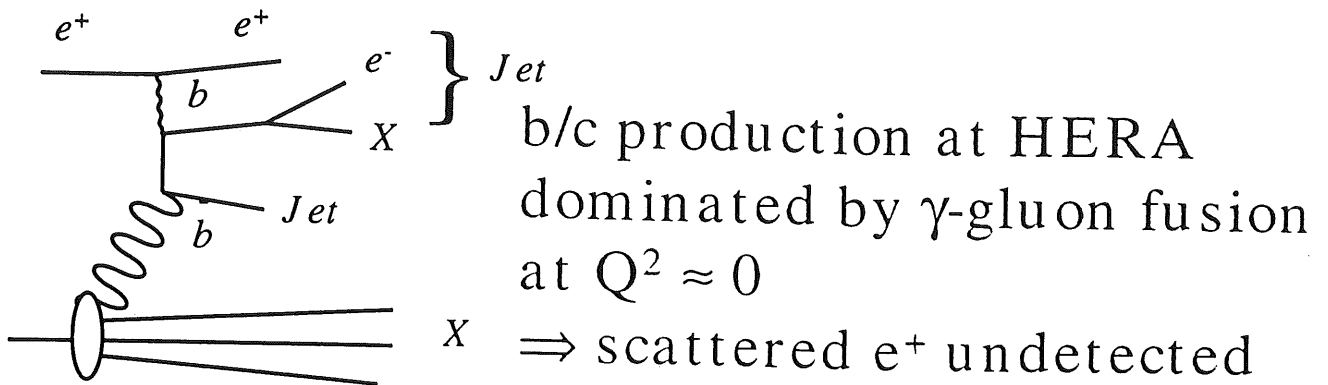


Data lie above
NLO calculations



In particular
in forward direction,
i.e. at high η^{D^*}

Photoproduction of Beauty



\Rightarrow look for electron from semileptonic b/c decay

using dE/dx in the CTD to tag beauty production

Photoproduction of Beauty (cont.)

$$Q^2 < 1 \text{ GeV}^2$$

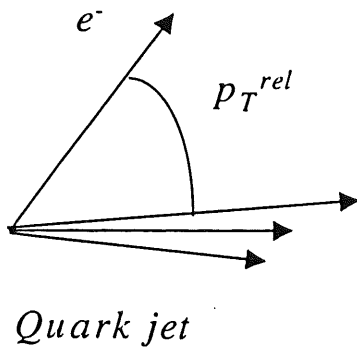
$$0.2 < y < 0.8$$

$$E_T^{jet1,2} > 7,6 \text{ GeV}$$

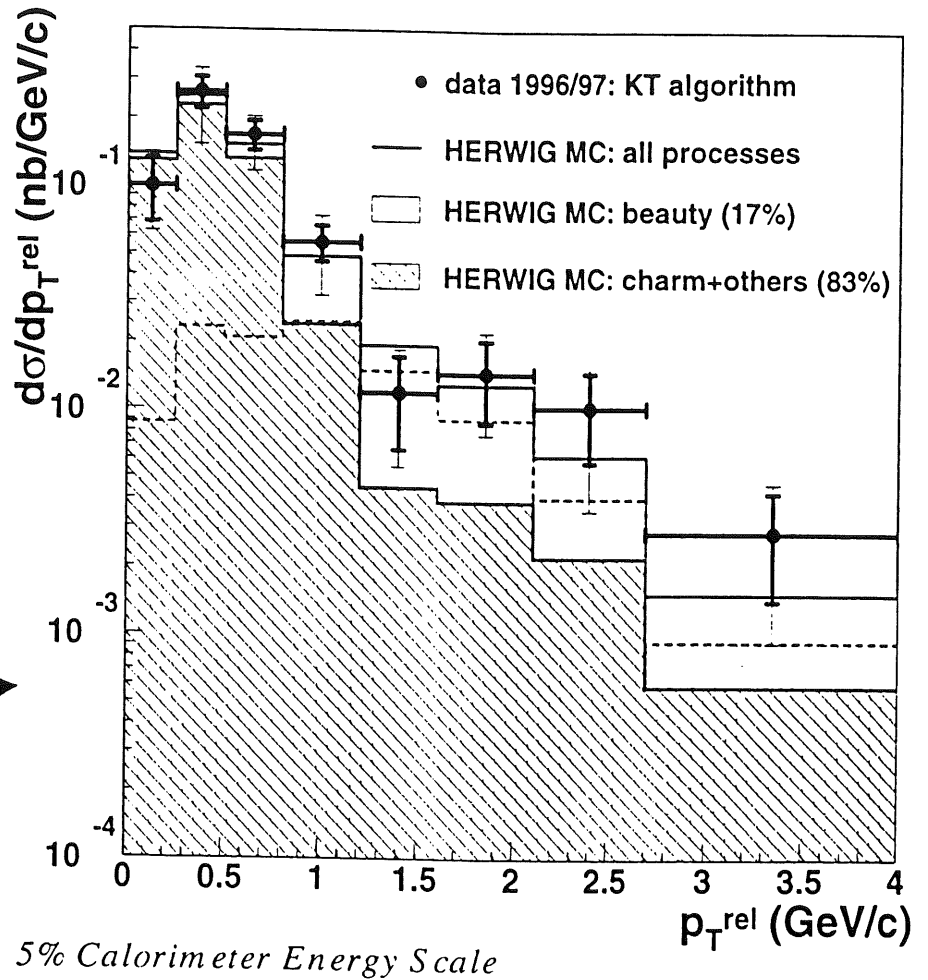
$$|\eta(jet)| < 2.4$$

$$p_T(e^-) > 1.6 \text{ GeV}/c$$

$$|\eta(e^-)| < 1.1$$



ZEUS PRELIMINARY (36.9 pb⁻¹)



- “other” are mostly Dalitz pairs
- ratios resolved/direct and other/c/b reasonably well described by HERWIG

$$\text{Fraction of beauty : } (20 \pm 6_{-7}^{+12}) \%$$

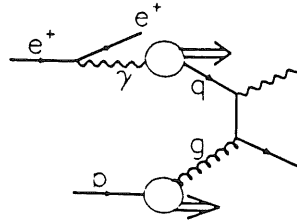
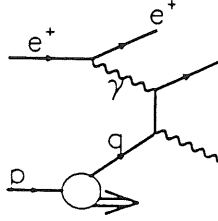
Visible cross section for 2 jets & 1 e⁻ from b-decay :

$$\sigma_{e^+p \rightarrow e^- + 2 \text{ jets} + X} = 39 \pm 11_{-15}^{+23} \text{ pb (preliminary)}$$

Factor of 2 higher than in HERWIG

Photoproduction of Prompt Photons

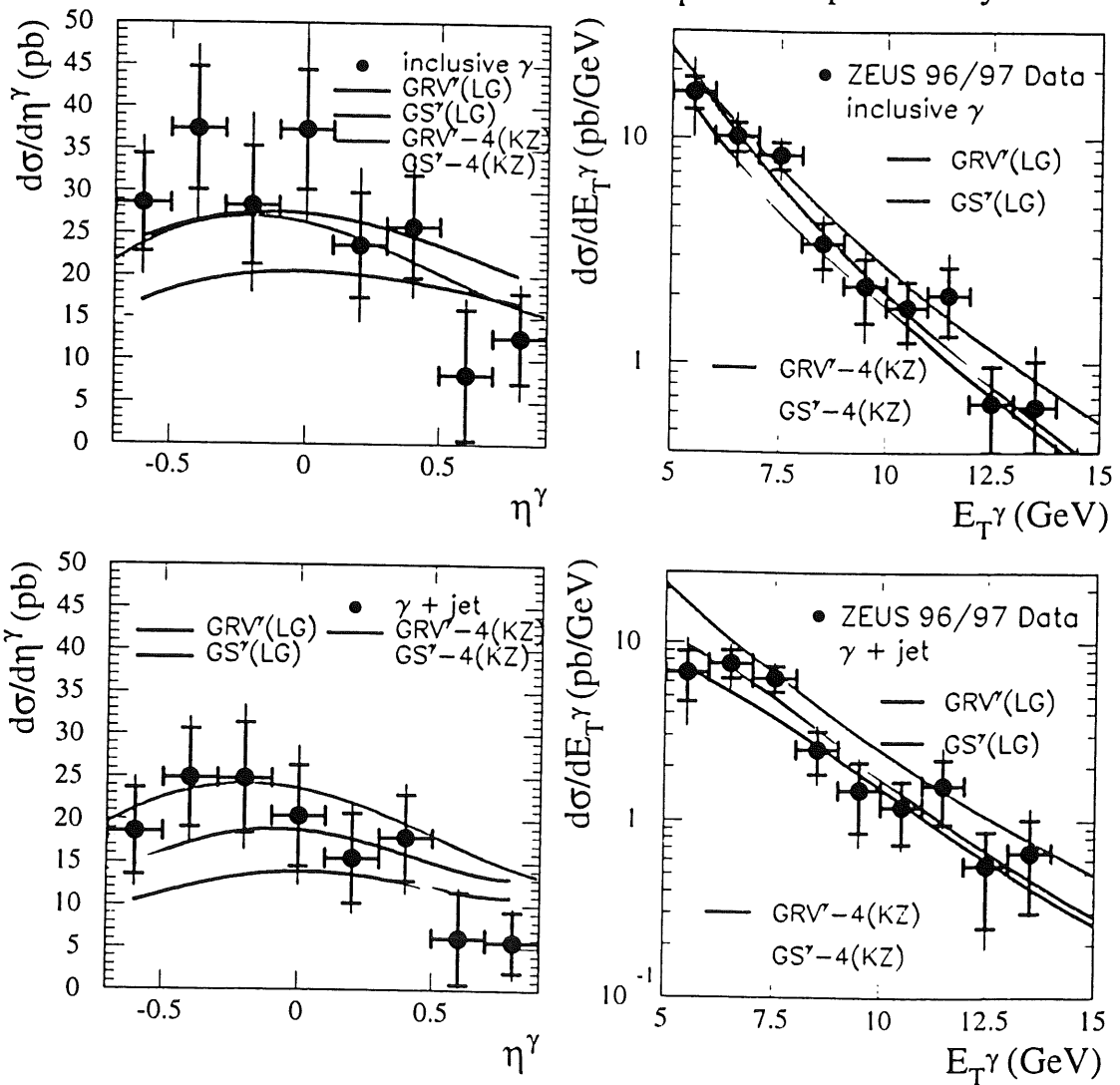
LO contributions from: Compton process and resolved contribution.



Inclusive direct photons
and direct photon +jet

$$5 < E_\gamma < 10 \text{ GeV}$$

Cross sections ($d\sigma/d\eta^\gamma, d\sigma/dE_{T,\gamma}$) ZEUS preliminary

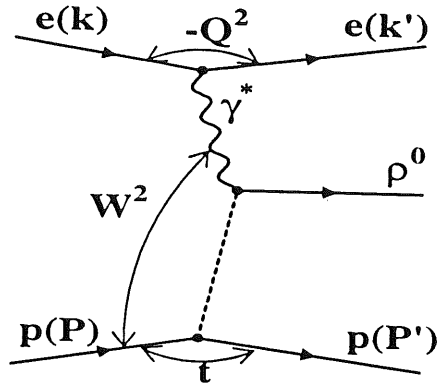


Generally good description by NLO calculations. GRV slightly preferred

Diffraction

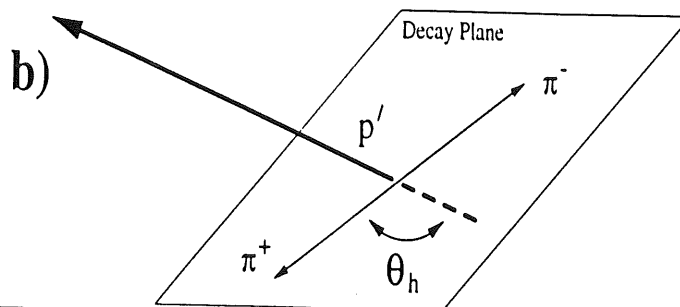
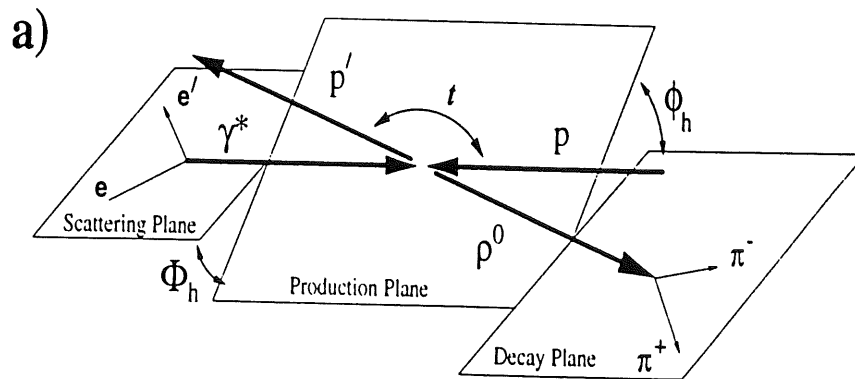
Diffraction : no exchange of quantum numbers except angular momentum and parity,
but dissociation of scattering particles into final state.

Exclusive vector meson production



In low energy data, s-channel helicity conservation (SCHC) seemed to be conserved.

Test SCHC hypothesis \Rightarrow measure angular distributions of vector meson decay particles.

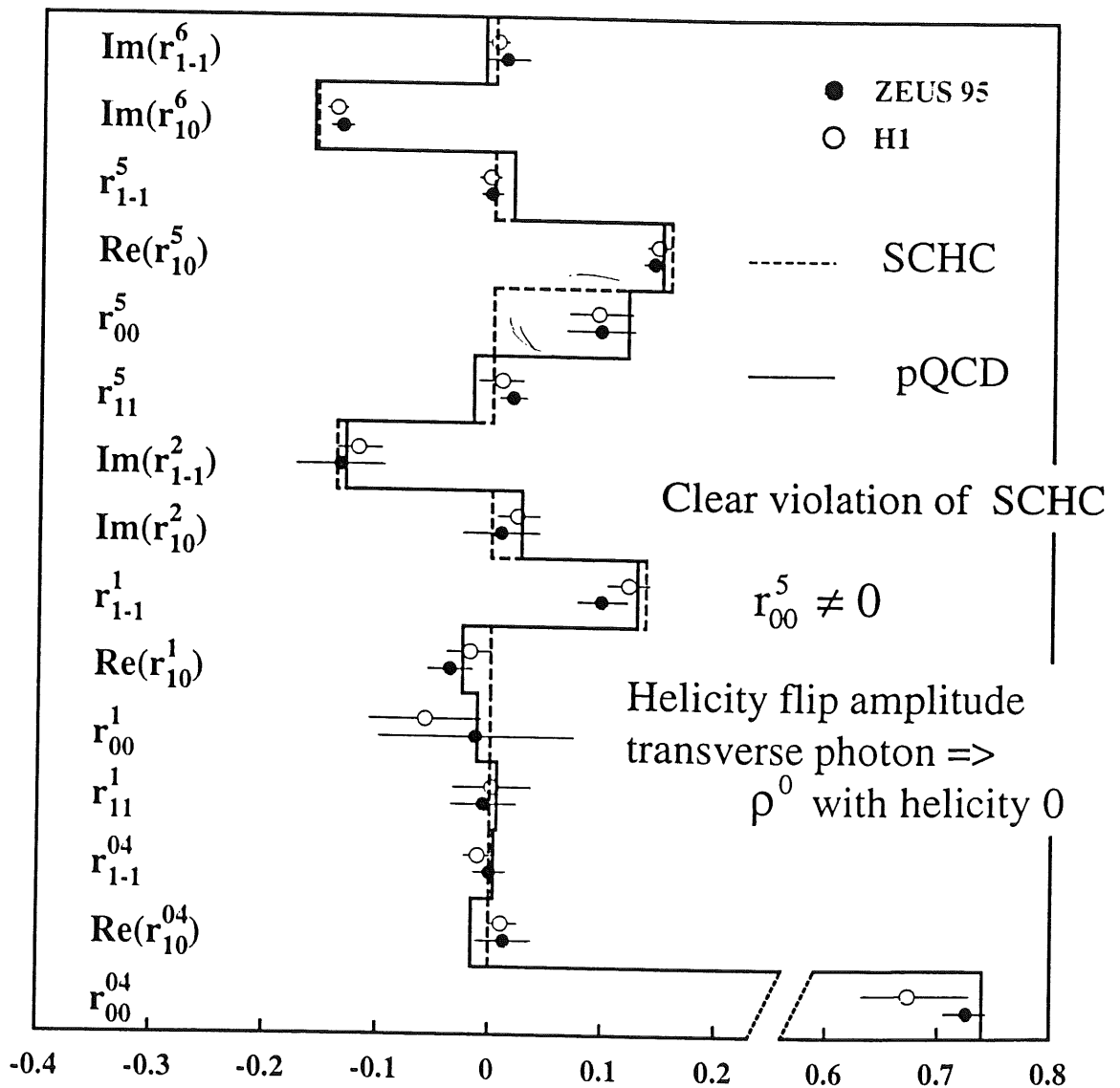


Spin Density Matrix

Parity conservation, hermitian spin density matrix =>

angular distribution of rho production and decay depends on 15 terms

ρ^0 production : $3 < Q^2 < 30 \text{ GeV}^2$; $40 < W < 120 \text{ GeV}$

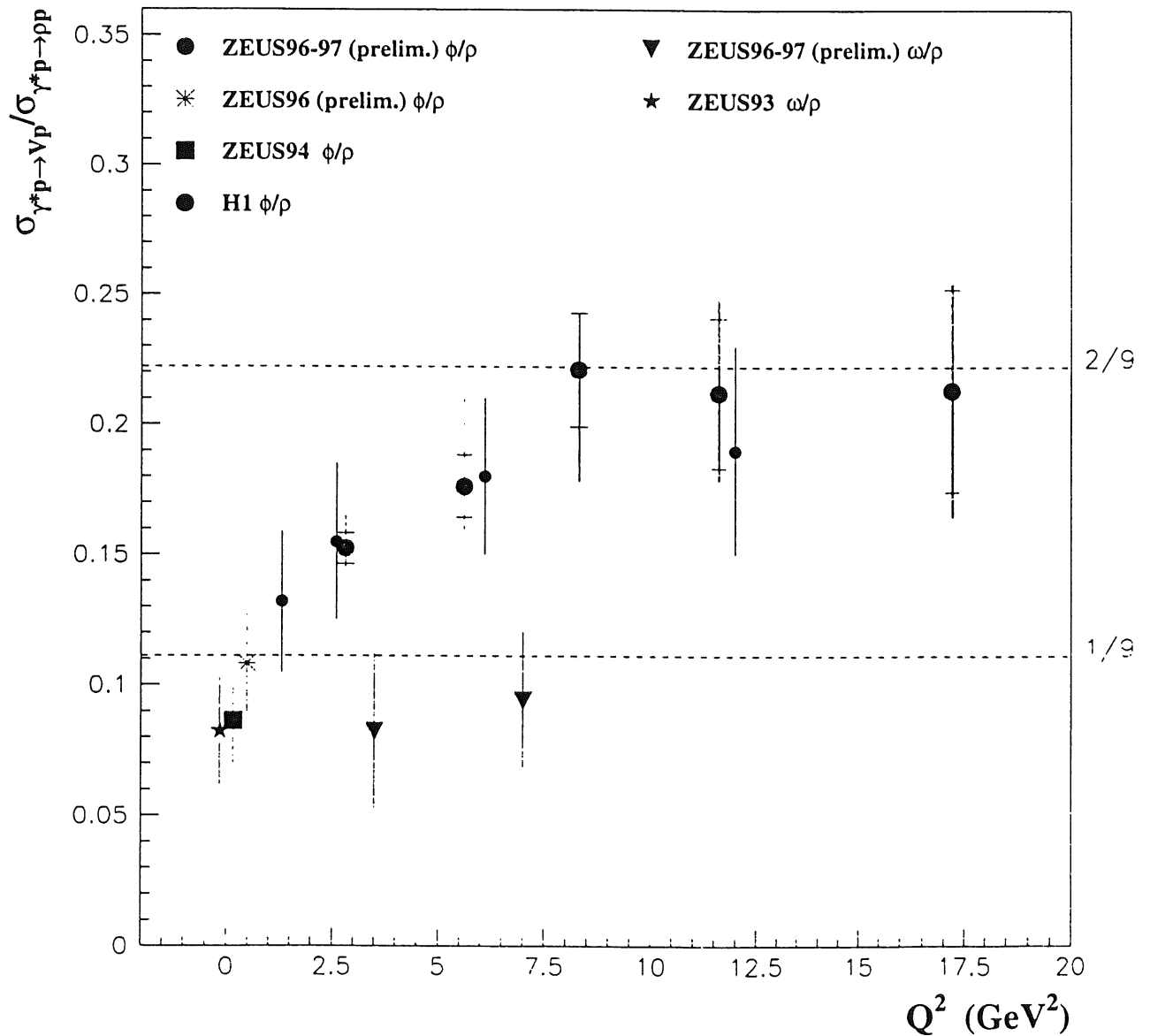


In BPC data at lower Q^2 , violation of SCHC is also seen.

Exclusive Vector Meson Production in DIS

$$e^+p \rightarrow e^+p\omega; \omega \rightarrow \pi^+\pi^-\pi^0; \pi^0 \rightarrow \gamma+\gamma$$

$$e^+p \rightarrow e^+p\phi; \phi \rightarrow K^+K^- \text{ and } \phi \rightarrow \pi^+\pi^-\pi^0$$



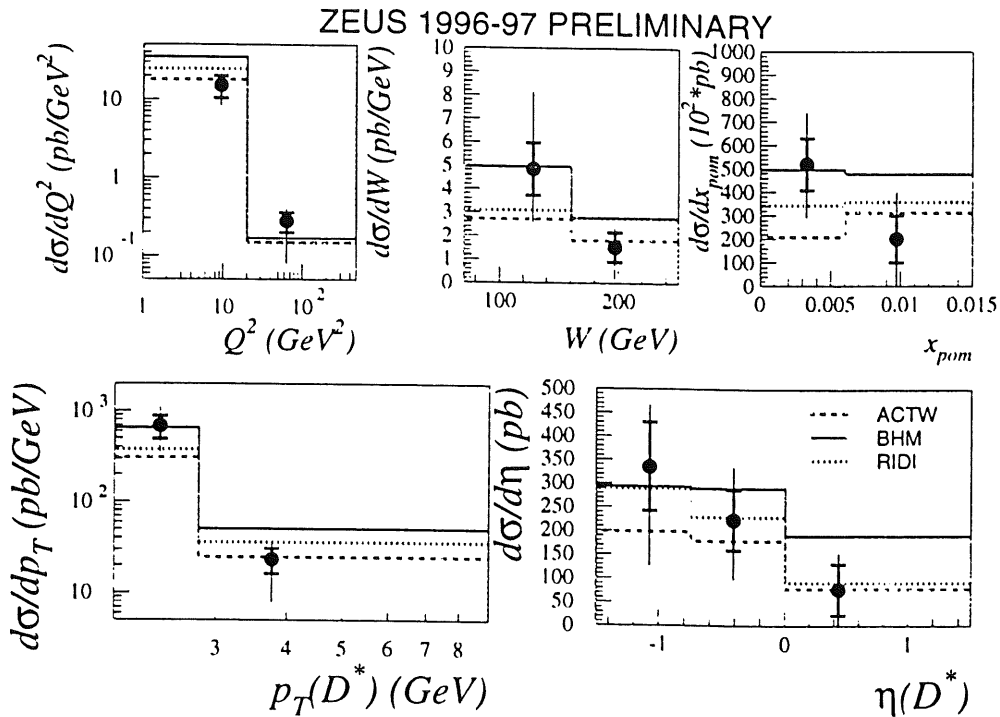
Ration of light vector meson production approaches U(4) limit with increasing Q^2 :

$$\rho : \omega : \phi = 9 : 1 : 2$$

Charm in Diffraction

Charm mass provides sufficiently hard scale => pQCD applicable

Results from $e^+p \rightarrow e^+pD^*X$; $D^* \rightarrow \pi D^0$; $D^0 \rightarrow K\pi$ have been shown at ICHEP98. New result from decay channel $D^0 \rightarrow K3\pi$ available in kinematic region : $1 < Q^2 < 600 \text{ GeV}^2$, $0.04 < y < 0.7$, $2 < p_T(D^*) < 9 \text{ GeV}^2$
 $|\eta(D^*)| < 1.5$, $x_p < 0.015$; $\beta < 0.8$



$$\sigma(e^+p \rightarrow e^+pD^*X) = 526 \pm 109(\text{stat.})^{+203}_{-239}(\text{syst.}) \text{ pb}$$

Interpolated to the $D^* \rightarrow K\pi$ kinematic region this is :

$$\sigma(e^+p \rightarrow e^+pX\pi K3\pi) = 398 \pm 83(\text{stat.})^{+154}_{-180}(\text{syst.}) \text{ pb}$$

Compare to

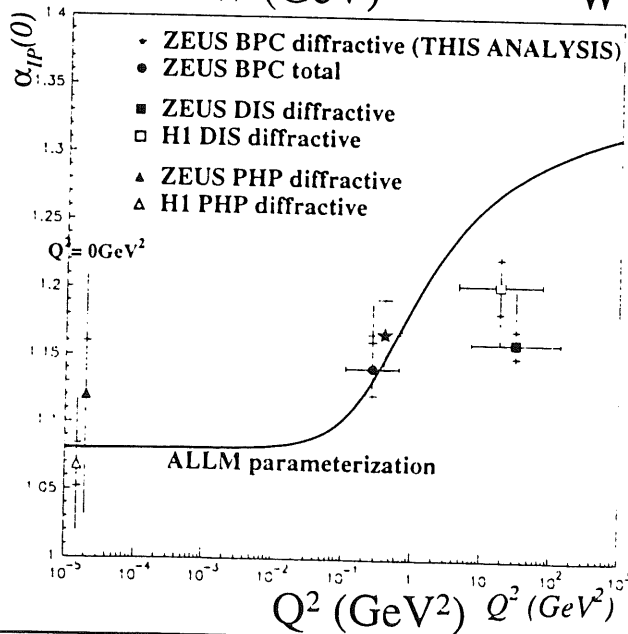
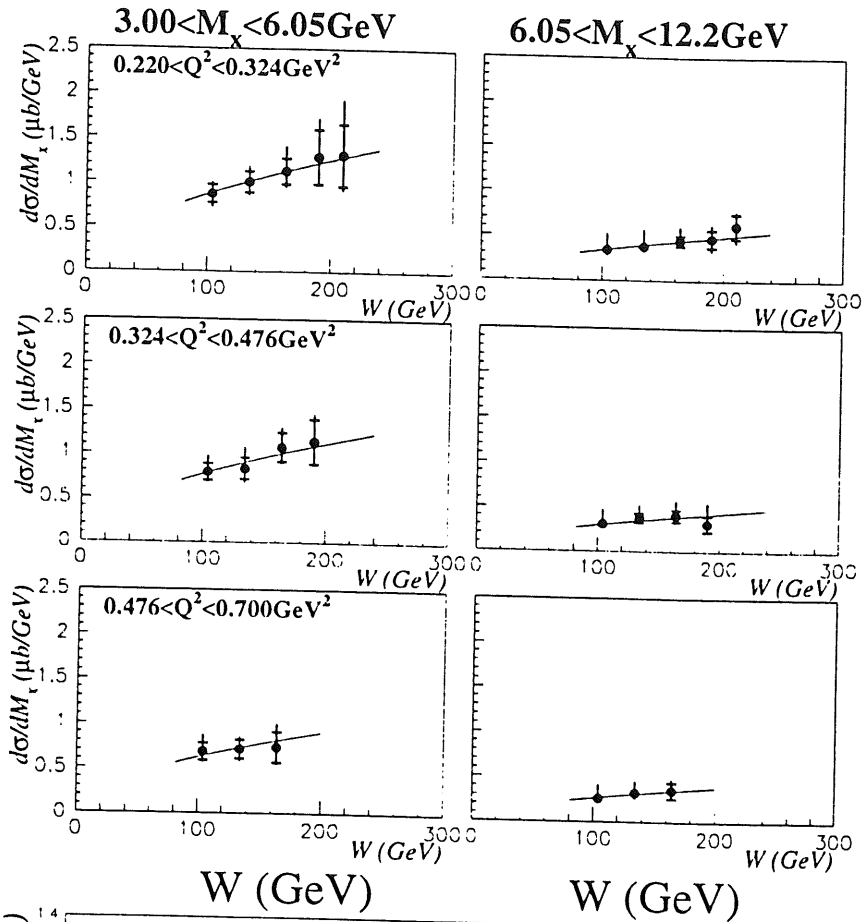
$$\sigma(e^+p \rightarrow e^+pX\pi K\pi) = 379 \pm 66(\text{stat.})^{+99}_{-140}(\text{syst.}) \text{ pb}$$

Ratio of diffractive D^* to total D^* production : $(8.9 \pm 2.4^{+1.7}_{-1.6}) \%$
 (from $D^* \rightarrow \pi(K3\pi)$ decay channel)

Diffractive Cross Section at low Q^2

Data : BPT tagged events

Statistical separation of diffractive events by $\ln M_x^2$ method



From the W dependence of the diffractive cross section the Pomeron trajectory is extracted.

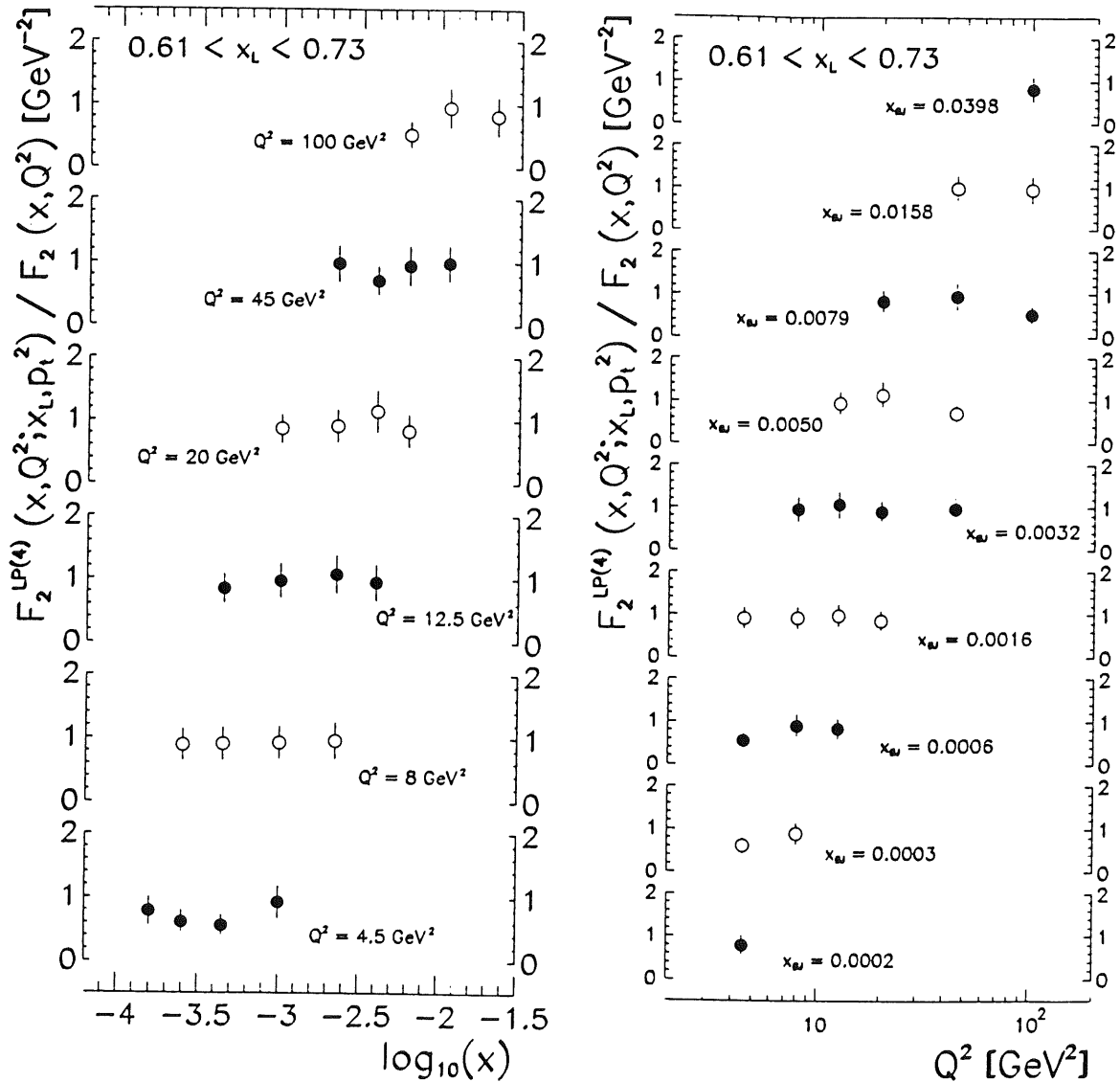
Consistent with result obtained BPC γ^*p total cross section.

Leading Protons

Look for leading protons in the LPS with $x_L < 0.97$.

Dominant contribution from Reggeon exchange : π and f^0 .

ZEUS PRELIMINARY 1995



The fraction of leading protons for $x_L < 0.97$ is only weakly dependent on x and Q^2 .

This confirms the factorization hypothesis.

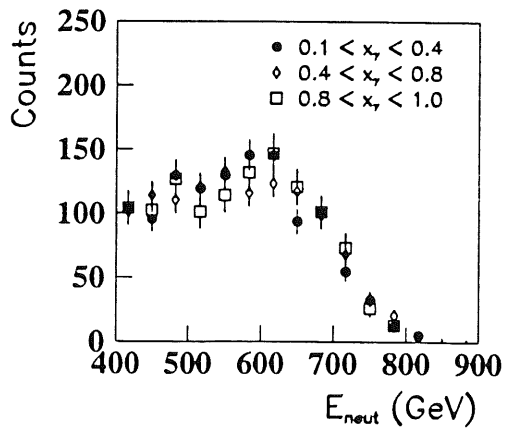
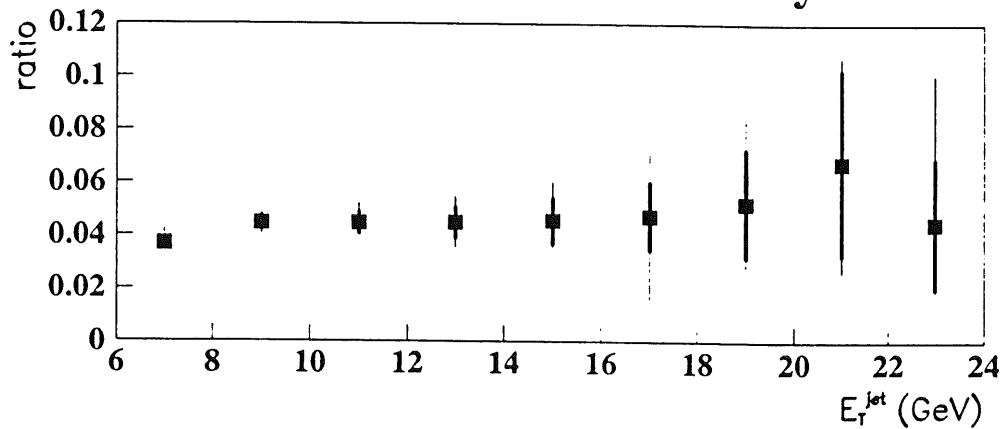
Similar results have been obtained for leading neutrons.

Leading Neutrons with Dijets

Photoproduction of events with dijets.
Events tagged by FNC if leading neutron present.

Determine $\text{ratio} = \frac{\text{dijets} + \text{leading neutron}}{\text{all dijets}}$

ZEUS 1995 Preliminary



Neutron energy spectrum for tagged events for different x_γ

Support of factorization hypothesis

Event Shapes in Diffraction

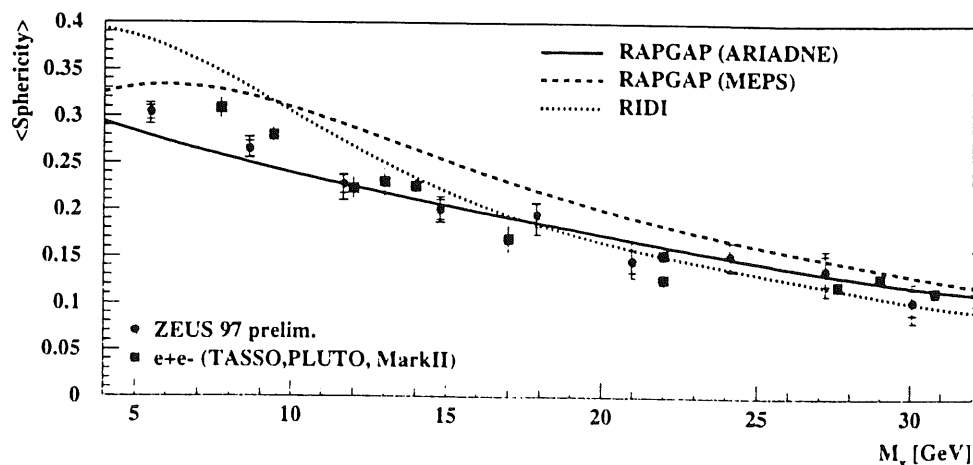
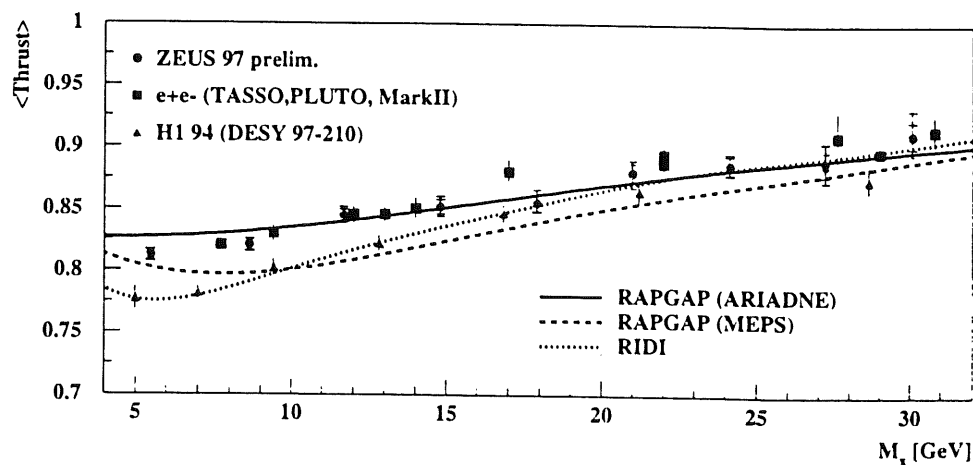
Scattered proton detected in Leading Proton Spectrometer (LPS).

Event sample : $4 \text{ GeV}^2 < Q^2 < 90 \text{ GeV}^2$; $4 \text{ GeV}^2 < M_x < 35 \text{ GeV}^2$

Transform hadronic final state into photon-pomeron center of mass system.

Calculate thrust and sphericity .

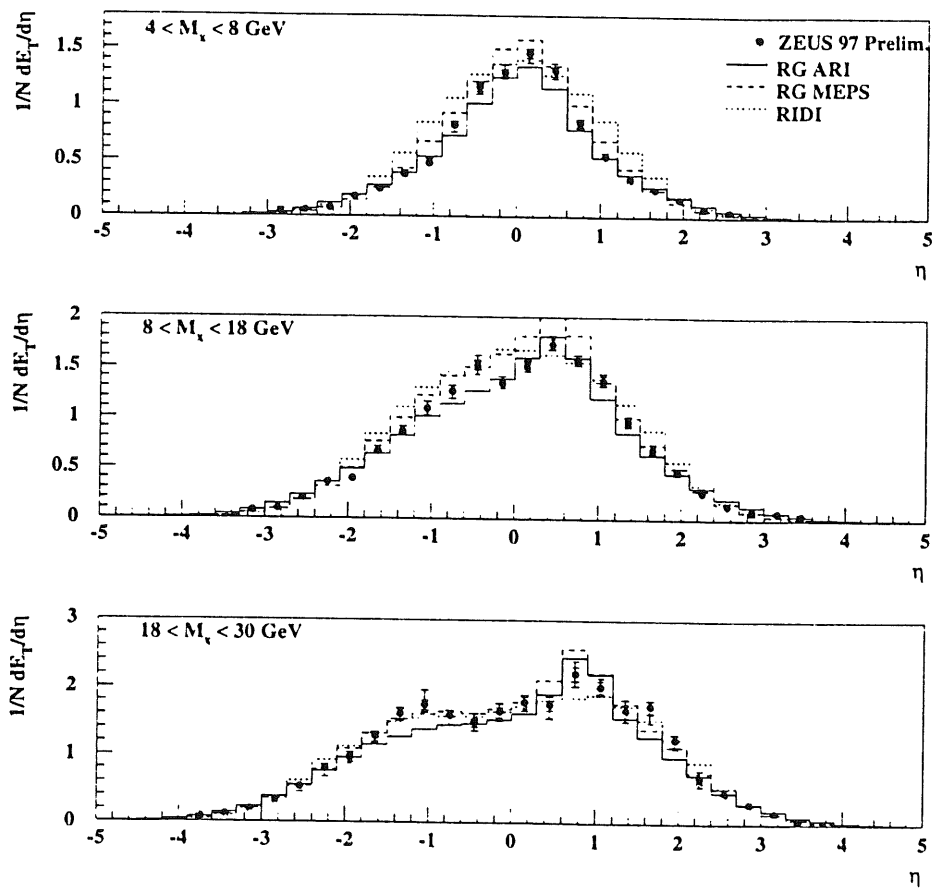
Average thrust and average sphericity as function of M_x



RIDI : MC program based on 2 gluon exchange

Event Shapes in Diffraction (cont.)

Transverse energy flow in photon-pomeron rest system



Development of jet structure as M_x increases

Summary

- The increased amount of data and instrumental improvements allow to increase the kinematical region accessible to measurements.
- At the the low Q^2 region, the data now come very close to photoproduction.
- At the high Q^2 region, we become sensitive to weak physics.
- The increased amount of data enables the study of jets in the final states in kinematical regions in which experimental uncertainties become smaller and the predictions of theoretical models are supposed to be more reliable.
- HERA switched to running with electrons since last year. First comparisons between e^+p and e^-p cross sections have been done. More can be expected at the end of this running period .
- Diffractive physics is still an interesting issue.